AIMS Mathematics, 11(11): 36948–36979.
DOI: 10.3934/math.20261427
Received: 07 July 2026
Revised: 03 October 2026
Accepted: 15 October 2026
Published: 09 November 2026

https://www.aimspress.com/journal/Math

Research article

Bogdanov–Takens codimension-2 bifurcation in a discrete predator–prey system with the generalized Holling type-III functional response and a strong Allee effect

Mirela Garić-Demirović[1,*], Dragana Kovačević[2], Mehmed Nurkanović[1] and Zehra Nurkanović[1]

[1] University of Tuzla, Department of Mathematics, Tuzla 75000, Bosnia and Herzegovina
[2] University of Sarajevo, Department of Mathematics, Sarajevo 71000, Bosnia and Herzegovina

* **Correspondence:** Email: mirela.garic@untz.ba.

Abstract: This work investigated the Bogdanov–Takens codimension-2 bifurcation in a discrete predator–prey model constructed by applying a combination of logarithmic discretization and the Euler method to a continuous system with a generalized Holling type-III functional response and a strong Allee effect. Using normal form theory, we explicitly derived parameter conditions for the existence of a positive equilibrium exhibiting a Bogdanov–Takens singularity. Numerical simulations were presented to illustrate the corresponding phase portraits and support the analytical results.

Keywords: difference equations; fixed point; codimension-2 bifurcation; Bogdanov–Takens bifurcation; predator–prey model
Mathematics Subject Classification: 39A28, 39A30, 37G10, 92D25

1. Introduction

The Bogdanov–Takens (BT) bifurcation is a codimension-2 phenomenon that arises at a degenerate equilibrium. It appears in continuous-time, time-delayed, and discrete-time predator–prey models with nonmonotonic functional responses. In discrete-time systems, it occurs when both eigenvalues of the Jacobian matrix at an interior equilibrium are equal to 1. The Bogdanov–Takens bifurcation reveals complex dynamical behavior and the underlying structure of predator-prey systems. It corresponds to a degeneracy of an equilibrium point at which local and global phenomena, including saddle-node bifurcation, Hopf bifurcation (or Neimark–Sacker bifurcation in discrete time), and homoclinic bifurcation, interact. In systems with nonlinear functional responses, the Bogdanov–Takens bifurcation represents an organizing center for system dynamics. The Bogdanov–Takens bifurcation, one of the most important codimension-2 bifurcations in dynamical systems theory, was originally introduced in the context of continuous models [2, 3, 7, 13, 24, 32]. The development of discrete-time models has

raised the question of how much of this intricate local structure persists under discretization. Early studies indicate that the Bogdanov–Takens bifurcation can also occur in discrete systems, particularly those obtained via discretization of continuous flows or arising as Poincaré maps. Moreover, discrete dynamics can preserve key topological features of continuous systems. For instance, the work of Kuznetsov, Savin, and Sedova (2009) [23] shows that discretization methods (such as the Euler method) can retain the Bogdanov–Takens structure, while also introducing additional phenomena, including resonances and more complicated stability boundaries. See also [16, 27].

Numerous studies on discrete models focus on codimension-1 bifurcations, such as transcritical and flip bifurcations at boundary equilibria, as well as Neimark–Sacker and period–doubling bifurcations at interior equilibria [4–6, 9, 10, 15, 17, 18, 20, 21, 26]. Most of these results concern predator–prey systems. Despite this progress, significantly fewer works address codimension-2 bifurcations, particularly the Bogdanov–Takens bifurcation. This bifurcation is relatively rare and among the most challenging to analyze. Consequently, any new results concerning the Bogdanov–Takens bifurcation in discrete predator–prey models are of considerable importance. Such results provide deeper insight into the structure of complex (including chaotic) dynamics and contribute to a better understanding of population behavior in ecological systems [1].

In this paper, the Bogdanov–Takens bifurcation is investigated in the context of a discrete predator–prey model obtained via a logarithmic discretization scheme. We examine how the interplay between a generalized Holling type-III functional response and a strong Allee effect can lead to the occurrence of a Bogdanov–Takens bifurcation and influence the system's dynamics. Our goal is to clarify the combined impact of these mechanisms on complex dynamical behaviors observed in discrete settings. Nonlinear predator–prey models are among the central objects of study in mathematical biology, originating from the classical works of Alfred J. Lotka [25] and Vito Volterra [31]. Building on this foundation, contemporary research has shown that incorporating more realistic biological mechanisms, such as complex functional responses and low-density effects, leads to significantly richer dynamics than those observed in classical models. In particular, the generalized Holling type-III functional response and the Allee effect introduce nonlinearities that can give rise to multistability, oscillations, and chaotic behavior. Discrete predator–prey models can exhibit richer dynamical behaviors than their continuous counterparts, including period-doubling cascades, quasi-periodic orbits, and chaos. For example, He and Li [14] identified complex dynamics in a discrete model with a Holling type-III response, including flip and Neimark–Sacker bifurcations. Similar phenomena are discussed in [34, 35]. Incorporating the Allee effect into predator–prey models introduces survival thresholds and bistability. Models with a strong Allee effect may exhibit multiple attractors, including bistability and tristability [28], with important implications for population persistence and extinction.

Our investigation builds on the work of Y. Zeng and P. Yu [34], who performed a dynamical analysis of a continuous-time predator–prey model with a generalized Holling type-III functional response and a strong Allee effect. They considered a general model, the so-called Gause-type predator–prey model [8, 11], of the form

$$\begin{aligned} \frac{dx}{dt} &= f(x)x - \varphi(x,y)y, \\ \frac{dy}{dt} &= c\varphi(x,y)y - g(y)y, \end{aligned}$$

with $x(0) \geq 0$, $y(0) \geq 0$, where $x = x(t)$ and $y = y(t)$ denote the prey and predator population

densities at time t, respectively. The functions f and g are positive and represent the prey growth rate and the predator mortality rate, respectively, when other species are absent from the ecosystem. The positive constant c determines the rate of prey conservation efficiency relative to the predator. In such models, the function $\varphi(x, y)$ is called the functional response and describes the rate at which a predator consumes prey as a function of their density. The choice of this function largely determines the qualitative behavior of the system. They employed the Holling type-III functional response for $\varphi(x, y)$, given by

$$\varphi(x, y) = \varphi(x) = \frac{Mx^2}{ax^2 + bx + 1}.$$

Here, $M > 0$ represents the predation rate coefficient, $a > 0$ characterizes the saturation effect at high prey densities, and b reflects the search efficiency, particularly influencing predation at low and intermediate prey densities. The parameter b may be negative, provided that suitable conditions (e.g., $b > -2\sqrt{a}$) are imposed to ensure that $ax^2 + bx + 1 > 0$ for $x > 0$. Consequently, $\lim_{x\to\infty} \varphi(x) = \frac{M}{a}$. The authors used

$$f(x) = r\left(1 - \frac{x}{K}\right)(x - e)$$

as a modified logistic growth function to incorporate the multiplicative Allee effect. Here, r denotes the intrinsic growth rate, K is the carrying capacity of the prey population x, and e denotes the threshold of the Allee effect. The constraint $|e| < K$ is typically assumed, and a strong Allee effect occurs when $0 < e < K$. The function g is taken to be $g(y) = d$, where d is a positive constant. The threshold of the Allee effect is assumed to be well below the carrying capacity [30], and the condition $0 < e < K/2$ is imposed on the model.

The model takes the following form:

$$\begin{aligned}
\frac{dx}{dt} &= rx\left(1 - \frac{x}{K}\right)(x - e) - \frac{Mx^2y}{ax^2 + bx + 1}, \\
\frac{dy}{dt} &= y\left(\frac{Mcx^2}{ax^2 + bx + 1} - d\right).
\end{aligned}$$

By introducing the following scaling:

$$x = KX, \quad y = \frac{rY}{M}, \quad \text{and} \quad \tau = rKt,$$

the system becomes

$$\begin{cases}
\frac{dX}{d\tau} = X\left((1 - X)(X - E) - \frac{XY}{AX^2+BX+1}\right), \\
\frac{dY}{d\tau} = Y\left(\frac{CX^2}{AX^2+BX+1} - D\right),
\end{cases} \tag{1.1}$$

where $A = aK^2$, $C = \frac{cMK}{r}$, $D = \frac{d}{rK}$, and $E = \frac{e}{K}$ are positive parameters, while $B = bK$, with the constraints $B > -2\sqrt{A}$ and $0 < E < \frac{1}{2}$. It is shown that the necessary conditions for the existence of a Bogdanov–Takens bifurcation are satisfied, as confirmed by numerical simulations. In particular, Theorem 2 states that a Bogdanov–Takens bifurcation may occur at an interior equilibrium, but no further analysis is provided.

This motivates the present work, in which we discretize the model and conduct a comprehensive analysis of the Bogdanov–Takens bifurcation in the resulting discrete system.

By applying a combination of logarithmic discretization and the Euler method to System (1.1), we obtain the discrete system

$$\begin{cases} x_{n+1} = x_n e^{h\left((1-x_n)(x_n-E)-\frac{x_n y_n}{Ax_n^2+Bx_n+1}\right)}, \\ y_{n+1} = y_n e^{h\left(\frac{Cx_n^2}{Ax_n^2+Bx_n+1}-D\right)}, \end{cases} \tag{1.2}$$

where A, C, and D are positive parameters, $B > -2\sqrt{A}$, and $0 < E < 1/2$.

In this paper, we demonstrate that both the strong Allee effect and the generalized Holling type-III functional response play distinct roles in the emergence of the Bogdanov–Takens bifurcation, acting in different ways but through their mutual interaction. The strong Allee effect determines the permissible location of the positive equilibrium point relative to the Allee threshold ($E < \overline{x}_{\pm} < 1$), while the generalized Holling type-III functional response provides a nonlinear feedback mechanism between the predator and prey populations. Through their interaction, they jointly determine the parameter conditions under which a 1:1 resonant degeneracy of the interior equilibrium occurs.

One additional specific feature of the considered model (1.2) is that both signs of the coefficient s appear in the normal form, $s = +1$ and $s = -1$, since there are very few papers with this case. This reveals the model's distinctive dynamical richness, with the emergence of distinct behaviors in the neighborhood of the BT point. Thus, our goal is to analyze the occurrence of the Bogdanov-Takens bifurcation and, in particular, to construct numerical visualizations of the cases shown in Figure 8.8 in [22, p. 322]). In fact, most studies analyzing this type of bifurcation merely refer to that figure without illustrating specific scenarios within their own models.

Although predator–prey models were originally developed in ecology, their mathematical structure naturally arises in modeling chemical reactions (for example, in the continuous models of glycolysis proposed in [29], and in the general framework of biochemical oscillations considered in [12]).

In this paper, we study whether System (1.2) undergoes a Bogdanov–Takens bifurcation. In Section 2, we give the existence and local stability of equilibrium points of System (1.2). In Section 3, we derive the parameter conditions under which a unique positive equilibrium becomes a 1:1 resonant fixed point of System (1.2). In Section 4, using the bifurcation theory established in [22, pp. 410–415], we analyze small parameter perturbations for which System (1.2) undergoes a Bogdanov–Takens bifurcation near this equilibrium. These results are then used in Section 5 to construct phase portraits via numerical simulations for representative parameter values.

2. Equilibrium points and local stability

We now consider the existence and local stability of equilibrium points of System (1.2). It is clear that the equilibrium points of System (1.2) are solutions of the following system of algebraic equations:

$$\begin{aligned} \overline{x} &= \overline{x} e^{h\left((1-\overline{x})(\overline{x}-E)-\frac{\overline{x}\overline{y}}{A\overline{x}^2+B\overline{x}+1}\right)}, \\ \overline{y} &= \overline{y} e^{h\left(\frac{C\overline{x}^2}{A\overline{x}^2+B\overline{x}+1}-D\right)}. \end{aligned}$$

Given the biological context of System (1.2), we are interested only in equilibrium points with non-negative coordinates. Direct verification shows that System (1.2) can have at most five equilibrium

points: three on the Ox-axis ($\mathbf{E}_0 = (0,0)$, $\mathbf{E}_1 = (E,0)$, $\mathbf{E}_2 = (1,0)$), which exist for all parameter values. The positive equilibrium points satisfy following system:

$$\begin{cases} (1-\overline{x})(\overline{x}-E) = \frac{\overline{x}\overline{y}}{A\overline{x}^2+B\overline{x}+1}, \\ \frac{C\overline{x}^2}{A\overline{x}^2+B\overline{x}+1} = D. \end{cases} \tag{2.1}$$

From the second equation of System (2.1), we get the equation

$$(C-AD)\overline{x}^2 - BD\overline{x} - D = 0,$$

whose solutions are

$$\overline{x}_{\pm} = \frac{BD \pm \sqrt{B^2D^2 + 4D(C-AD)}}{2(C-AD)}$$

with $C \neq AD$, and

$$\overline{x}_{+} = -\frac{1}{B}$$

for $C = AD$.

From the first equation of System (2.1), we obtain that $\overline{y}$ is of the form

$$\overline{y} = \frac{(1-\overline{x})(\overline{x}-E)}{\overline{x}}\left(A\overline{x}^2 + B\overline{x} + 1\right) = \frac{C}{D}\overline{x}(1-\overline{x})(\overline{x}-E), \tag{2.2}$$

which is positive if $E < \overline{x} < 1$. There are at most two positive equilibrium points (interior equilibria), $\mathbf{E}_{3\pm} = (\overline{x}_{\pm}, \overline{y}_{\pm})$, subject to the conditions listed in Table 1. In Table 1, we use the following notation:

$$P(x) = (C-AD)x^2 - BDx - D, \quad \Delta = B^2D^2 + 4D(C-AD),$$
$$\overline{x}_{\pm} = \frac{BD \pm \sqrt{\Delta}}{2(C-AD)}, \quad \overline{y} = \frac{C\overline{x}(1-\overline{x})(\overline{x}-E)}{D}, \quad x_s = \frac{BD}{2(C-AD)}.$$

Conditions						Points
$C > AD$	$-2\sqrt{A} < B$		$P(E) < 0$	$P(1) > 0$		$\mathbf{E}_{3+}$
$C = AD$	$\max\left\{-2\sqrt{A}, -\frac{1}{E}\right\} < B < -1$					$\left(-\frac{1}{B}, \overline{y}\right)$
$C < AD$	$\triangle = 0$	$\max\left\{-2\sqrt{A}, -\frac{2}{E}\right\} < B < -2$				$\left(-\frac{2}{B}, \overline{y}\right)$
	$\triangle > 0$	$-2\sqrt{A} < B < 0$	$P(E) > 0$	$P(1) < 0$		$\mathbf{E}_{3-}$
			$P(E) < 0$	$P(1) > 0$		$\mathbf{E}_{3+}$
			$P(E) < 0$	$P(1) < 0$	$E < x_s < 1$	$\mathbf{E}_{3-}, \mathbf{E}_{3+}$

Table 1. Conditions for the existence of positive equilibrium points.

Note that when $C < AD$, $\Delta = 0$, and $\max\left\{-2\sqrt{A}, -\frac{2}{E}\right\} < B < -2$, the equilibria $\mathbf{E}_-$ and $\mathbf{E}_+$ coincide, merging into a single positive equilibrium where $\overline{x} = -\frac{2}{B}$.

We will now turn our attention to analyzing the local stability of these equilibrium points. The map associated with System (1.2) has the following form:

$$F(x,y) = \begin{pmatrix} xe^{h\left((1-x)(x-E)-\frac{xy}{Ax^2+Bx+1}\right)} \\ ye^{h\left(\frac{Cx^2}{Ax^2+Bx+1}-D\right)} \end{pmatrix}. \tag{2.3}$$

The Jacobian matrix of (2.3) has the form

$$J_F(x,y) = \begin{pmatrix} \kappa e^{h\left((1-x)(x-E)-\frac{xy}{Ax^2+Bx+1}\right)} & -\frac{hx^2e^{h\left((1-x)(x-E)-\frac{xy}{Ax^2+Bx+1}\right)}}{Ax^2+Bx+1} \\ \frac{xyh(Bx+2)Ce^{h\left(\frac{Cx^2}{Ax^2+Bx+1}-D\right)}}{\left(Ax^2+Bx+1\right)^2} & e^{h\left(\frac{Cx^2}{Ax^2+Bx+1}-D\right)} \end{pmatrix},$$

where

$$\kappa = 1 + hx\left(1 + E - 2x + y\frac{Ax^2-1}{\left(Ax^2+Bx+1\right)^2}\right).$$

Proposition 1. *The equilibrium point* $\mathbf{E}_0 = (0,0)$ *of System (1.2) is locally asymptotically stable.*

Proof. This follows directly from the Jacobian matrix at point $\mathbf{E}_0$:

$$J_F(\mathbf{E}_0) = \begin{pmatrix} e^{-hE} & 0 \\ 0 & e^{-hD} \end{pmatrix},$$

whose eigenvalues are $0 < \lambda_1 = e^{-hE} < 1$ and $0 < \lambda_2 = e^{-hD} < 1$. □

Proposition 2. *The equilibrium point* $\mathbf{E}_1 = (E,0)$ *of System (1.2) is:*

i) a saddle point if $\frac{CE^2}{AE^2+BE+1} < D$;

ii) non-hyperbolic if $\frac{CE^2}{AE^2+BE+1} = D$;

iii) a repeller if $\frac{CE^2}{AE^2+BE+1} > D$.

Proof. Since $0 < E < \frac{1}{2}$ and the Jacobian matrix

$$J_F(\mathbf{E}_1) = \begin{pmatrix} 1 + hE(1-E) & -\frac{hE^2}{AE^2+BE+1} \\ 0 & e^{h\left(\frac{CE^2}{AE^2+BE+1}-D\right)} \end{pmatrix}$$

has the eigenvalues $\lambda_1 = 1 + hE(1-E)$ and $\lambda_2 = e^{h\left(\frac{CE^2}{AE^2+BE+1}-D\right)}$, then $\lambda_1 > 1$ for all $h > 0$, and

$$\lambda_2 \begin{cases} < 1 \text{ if } \frac{CE^2}{AE^2+BE+1} < D, \\ = 1 \text{ if } \frac{CE^2}{AE^2+BE+1} = D, \\ > 1 \text{ if } \frac{CE^2}{AE^2+BE+1} > D. \end{cases}$$

□

	$D < \widehat{D}$	$D = \widehat{D}$	$D > \widehat{D}$
$h < \widehat{h}$	SP	NH (codim-1)	LAS
$h = \widehat{h}$	NH (codim-1)	NH (codim-2)	NH (codim-1)
$h > \widehat{h}$	R	NH (codim-1)	SP

Table 2. Properties of the equilibrium $\mathbf{E}_2 = (1, 0)$ (SP–"a saddle point", R–"a repeller", NH–"non-hyperbolic").

Proposition 3. *Let $\widehat{h} = \frac{2}{1-E}$ and $\widehat{D} = \frac{C}{A+B+1}$. The local stability of the equilibrium point $\mathbf{E}_2 = (1, 0)$, depending on the parameter values, is shown in Table 2.*

Proof. This follows from the fact that the Jacobian matrix at the equilibrium point $\mathbf{E}_2 = (1, 0)$ has the form

$$J_F(\mathbf{E}_2) = \begin{pmatrix} 1 - h(1 - E) & -\frac{h}{A+B+1} \\ 0 & e^{h\left(\frac{C}{A+B+1} - D\right)} \end{pmatrix},$$

with the eigenvalues $\lambda_1 = 1 - h(1 - E) < 1$ and $\lambda_2 = e^{h\left(\frac{C}{A+B+1} - D\right)}$. □

Proposition 4. *Assume that all conditions for the existence of the equilibrium points $\mathbf{E}_{3+}$, $\mathbf{E}_{3-}$, and $\left(-\frac{1}{B}, \overline{y}\right)$ in Table 1 are satisfied. Then the following statements hold:*

a) The equilibrium point $\mathbf{E}_{3-}$ is unstable.

b) The equilibrium points $\mathbf{E}_{3+}$ and $\left(-\frac{1}{B}, \overline{y}\right)$ are locally asymptotically stable if and only if

$$Q(\overline{x}_3)h^2 + 2R(\overline{x}_3)h + 4 > 0 \ \text{ and } \ Q(\overline{x}_3)h + R(\overline{x}_3) < 0,$$

where $\overline{x}_3 = \overline{x}_+$ or $\overline{x}_3 = -\frac{1}{B}$ and

$$Q(x) = \frac{(1 - x)(x - E)(Bx + 2)D^2}{Cx^2}, \quad R(x) = x(1 + E - 2x) + \frac{D\left(Ax^2 - 1\right)(1 - x)(x - E)}{Cx^2}.$$

Proof. Let $\mathbf{E}_3 = (\overline{x}_3, \frac{C}{D}\overline{x}_3(1 - \overline{x}_3)(\overline{x}_3 - E))$ generally denote a positive equilibrium point, where $E < \overline{x} < 1$. Since

$$\frac{C\overline{x}_3^2}{A\overline{x}_3^2 + B\overline{x}_3 + 1} = D,$$

the Jacobian matrix at that equilibrium point is

$$J_F(\mathbf{E}_3) = \begin{pmatrix} 1 + h\overline{x}_3\left(1 + E - 2\overline{x}_3 + \frac{D}{C\overline{x}_3^3}\left(A\overline{x}_3^2 - 1\right)(1 - \overline{x}_3)(\overline{x}_3 - E)\right) & -\frac{hD}{C} \\ \frac{hD}{\overline{x}_3^2}(1 - \overline{x}_3)(\overline{x}_3 - E)(B\overline{x}_3 + 2) & 1 \end{pmatrix},$$

from which

$$TrJ_F(\mathbf{E}_3) = R(\overline{x}_3)h + 2$$

and

$$\det J_F(\mathbf{E}_3) = Q(\overline{x}_3)h^2 + R(\overline{x}_3)h + 1.$$

The equilibrium point $\mathbf{E}_3$ is locally asymptoticaly stable if and only if

$$1 - trJ_F(\mathbf{E}_3) + \det J_F(\mathbf{E}_3) = Q(\overline{x}_3)h^2 > 0,$$
$$1 + trJ_F(\mathbf{E}_3) + \det J_F(\mathbf{E}_3) = Q(\overline{x}_3)h^2 + 2R(\overline{x}_3)h + 4 > 0,$$
$$1 - \det J_F(\mathbf{E}_3) = -h\left(R(\overline{x}_+) + hQ(\overline{x}_+)\right) > 0.$$

a) Since

$$B\overline{x}_- + 2 = \frac{B^2D - B\sqrt{\Delta}}{2(C - AD)} + 2 = \frac{B^2D - B\sqrt{\Delta} + 4(C - AD)}{2(C - AD)}$$
$$= \frac{B^2D - B\sqrt{\Delta} + \frac{\Delta - B^2D^2}{D}}{2(C - AD)} = \frac{\sqrt{\Delta}\left(-BD + \sqrt{\Delta}\right)}{2D(C - AD)} < 0$$

($C - AD < 0$ and $B < 0$), then $Q(\overline{x}_-) < 0$, which implies that the condition $1 - trJ_F(\mathbf{E}_{3-}) + \det J_F(\mathbf{E}_{3-}) > 0$ is violated. This means that $\mathbf{E}_{3-}$ is unstable.
b) Since $B\left(-\frac{1}{B}\right) + 2 = 1 > 0$ and

$$B\overline{x}_+ + 2 = \frac{\sqrt{\Delta}\left(BD + \sqrt{\Delta}\right)}{2D(C - AD)} > 0,$$

we obtain that $Q(\overline{x}_+) > 0$. Condition $R(\overline{x}_+) + hQ(\overline{x}_+) < 0$ implies that $R(\overline{x}_+) < 0$ and $h < -\frac{R(\overline{x}_+)}{Q(\overline{x}_+)}$. This indicates that $\mathbf{E}_{3+}$ can be stable and that the stability of the equilibrium $\mathbf{E}_{3+}$ depends on h, as we confirmed through experiments with specific examples. This completes the proof. □

The question of the existence of an invariant set for System (1.2) is of particular importance; therefore, we shall now examine it in greater detail.

It follows from (1.2) that the first quadrant is positively invariant for that system, since the exponential terms are positive and

$$x_n \geq 0, \;\; y_n \geq 0 \Longrightarrow x_{n+1} \geq 0, \;\; y_{n+1} \geq 0.$$

Since, under the assumption that $B > -2\sqrt{A}$, the expression $Ax^2 + Bx + 1$ is positive for all $x \geq 0$ and the predatory term $\frac{x}{Ax^2+Bx+1}$ is non-negative. Thus, for $x_n \geq 1$, $x_{n+1} \leq x_n$, $n = 0, 1, ...$, and, in particular, when $x_n = 1$,

$$x_{n+1} = e^{-\frac{hy_n}{A+B+1}} \leq 1.$$

Although $[0, 1]$ is not an invariant interval for the prey population x without additional restrictions, since x_{n+1} can exceed 1 when $E < x_{n+1} < 1$, if $0 < x_n \leq E$, then $(1 - x_n)(x_n - E) \leq 0$. Consequently, $x_{n+1} \leq x_n \leq E$, which means that the set $[0, E] \times [0, \infty)$ is positively invariant for System (1.2).

A more precise result is given by the following proposition.

Proposition 5. *If*

$$\frac{CE^2}{AE^2 + BE + 1} < D \text{ for } B \geq -\frac{2}{E}$$

or

$$\frac{4C}{4A - B^2} < D \text{ for } -2\sqrt{A} < B < -\frac{2}{E},$$

then the following statements hold:

i) For every $N > 0$, the rectangle $[0, E] \times [0, N]$ is a positively invariant set for System (1.2).

ii) The rectangle $[0, E] \times [0, N]$ is an absorbing set for System (1.2), for $x_0 \in [0, E]$; that is, every such solution eventually enters $[0, E] \times [0, N]$.

iii) The set $\mathcal{P} = [0, E] \times [0, \infty)$ is a positively invariant set for System (1.2), and $\mathcal{P} \setminus \{(E, 0)\}$ is contained in the basin of attraction of $\mathbf{E}_0 = (0, 0)$.

Proof. Let $g(x) = \frac{Cx^2}{Ax^2+Bx+1}$. Note that

$$\max_{x\in[0,E]} \frac{Cx^2}{Ax^2 + Bx + 1} = \begin{cases} \frac{CE^2}{AE^2+BE+1}, & \text{if } B \geq -\frac{2}{E}, \\ \frac{4C}{4A-B^2}, & \text{if } -2\sqrt{A} < B < -\frac{2}{E}. \end{cases}$$

i) As we can see, $[0, E]$ is a positively invariant interval for the prey population x. Under the given conditions, we have

$$y_{n+1} \leq y_n e^{h\left(\max\limits_{x\in[0,E]} g(x)-D\right)} \leq y_n.$$

Hence, if $x_0 \in [0, E]$ and $y_0 \leq N$, then $x_n \in [0, E]$ and $y_n \leq N$ for all $n \geq 0$. Therefore, $[0, E] \times [0, N]$ is positively invariant.

ii) Let $G = \max\limits_{x\in[0,E]} g(x)$. Generally, for $x_n \in [0, E]$, the second equation of System (1,2) gives

$$y_{n+1} \leq y_n e^{h(G-D)}.$$

Consequently,

$$0 \leq y_n \leq y_0 e^{nh(G-D)} \to 0 \text{ as } n \to \infty.$$

Hence, there exists a sufficiently large n such that $y_n \leq N$. Since $x_n \in [0, E]$, it follows that $(x_n, y_n) \in [0, E] \times [0, N]$ for all sufficiently large n.

iii) Part i) implies that $\mathcal{P} = [0, E] \times [0, \infty)$ is a positively invariant set for System (1.2). We have just shown that, under the given assumptions, y_n tends to zero. Since the first equation of System (1.2) implies that $0 \leq x_{n+1} \leq x_n$ whenever $x_n \in [0, E]$, the sequence $\{x_n\}$ is nonincreasing and bounded below; hence, it converges to a limit L. Taking the limit as $n \to \infty$ in the first equation of System (1.2), we obtain

$$L = Le^{h(1-L)(L-E)}. \tag{2.4}$$

Let us prove that $L = 0$. Suppose, to the contrary, that $L > 0$. Then equation (2.4) implies $L = E$ or $L = 1$. Since $x_n \leq E$ for all n, $L = 1$ is impossible. Moreover, if $L = E$, then, because $\{x_n\}$ is nonincreasing, we must have $x_n = E$ for all n. This is possible only when $(x_0, y_0) = (E, 0)$. Therefore, for $(x_0, y_0) \in \mathcal{P} \setminus \{(E, 0)\}$, we necessarily have $L = 0$. Consequently, $\lim\limits_{n\to\infty} (x_n, y_n) = (0, 0)$, which means that $\mathcal{P} \setminus \{(E, 0)\}$ is contained in the basin of attraction of the equilibrium $\mathbf{E}_0$. □

Remark 6. *The biological significance of Proposition 5 is as follows: even when the prey population is initially at the Allee threshold (E), the presence of predators ($y_0 > 0$) causes the prey population to fall below this threshold in the next step. Thereafter, both populations tend toward extinction, that is, $x_n \to 0$ and $y_n \to 0$. Thus, in the present model, a prey population initially located exactly at the Allee threshold cannot persist in the presence of predators. Once the prey population falls below the Allee threshold, the model predicts its subsequent decline toward extinction, together with the extinction of the predator population.*

3. 1:1 resonant equilibrium point

In particular, we now determine the conditions for the existence of an interior fixed point with a 1:1 strong resonance.

Two values $\overline{x}_{\pm}$ merge into one, $\overline{x}$, if $B^2D + 4(C - AD) = 0$, i.e., if

$$D = D^* = \frac{4C}{4A - B^2},$$

then we obtain

$$\overline{x} = -\frac{2}{B}.$$

This implies that $\overline{x}$ is positive if and only if $B < 0$.

Notice that $\overline{y} > 0$ only if $\overline{x} \in (E, 1)$, where $E \in \left(0, \frac{1}{2}\right)$. For $D = D^*$, from (2.2), we obtain

$$\overline{y} = \frac{\left(4A - B^2\right)(BE + 2)(B + 2)}{2B^3} > 0, \quad B \in \left(-\frac{2}{E}, -2\right). \tag{3.1}$$

Notice that $B^2 - 4A < 0$ and $B \in \left(-\frac{2}{E}, -2\right)$ imply $A > 1$.

The Jacobian matrix of the map F defined by (2.3) in a positive equilibrium $\mathbf{E}_3 = (\overline{x}, \overline{y})$ has the form

$$J_F(\mathbf{E}_3) = \begin{pmatrix} 1 + h\overline{x}\left(1 + E - 2\overline{x} + \overline{y}\frac{A\overline{x}^2 - 1}{\left(A\overline{x}^2 + B\overline{x} + 1\right)^2}\right) & -h\frac{D}{C} \\ h\frac{(B\overline{x}+2)\overline{y}D^2}{C\overline{x}^3} & 1 \end{pmatrix}. \tag{3.2}$$

Then, $J_F(\mathbf{E}_3)$ has both eigenvalues equal to 1, i.e., $\mathbf{E}_3$ is a 1:1 resonant fixed point if $Tr\left(J_F(\mathbf{E}_3)\right) = 2$ and $\det\left(J_F(\mathbf{E}_3)\right) = 1$. The equation $Tr\left(J_F(\mathbf{E}_3)\right) = 2$ is equivalent to

$$1 + E - 2\overline{x} + \overline{y}\frac{A\overline{x}^2 - 1}{\left(A\overline{x}^2 + B\overline{x} + 1\right)^2} = 0. \tag{3.3}$$

By using (3.3), then from (3.2), we obtain

$$J_F(\mathbf{E}_3) = \begin{pmatrix} 1 & -h\frac{D}{C} \\ h\frac{(B\overline{x}+2)\overline{y}D^2}{C\overline{x}^3} & 1 \end{pmatrix}, \tag{3.4}$$

from which

$$\det\left(J_F(\mathbf{E}_3)\right) = 1 + h^2\frac{(B\overline{x} + 2)\overline{y}D^3}{C^2\overline{x}^3}.$$

Now,

$$\det\left(J_F(\mathbf{E}_3)\right) = 1 \Longleftrightarrow \overline{x} = x^* = -\frac{2}{B}. \tag{3.5}$$

For $\overline{x} = x^* = -\frac{2}{B}$, from (3.3), we get

$$Tr\left(J_F(\mathbf{E}_3)\right) = 2 \Longleftrightarrow -\frac{4B + 4BE + B^2E + 12}{2B} = 0,$$

which implies that $E = E^* = -\frac{4(B+3)}{B(B+4)}$. Then, for $E = E^*$, from (3.1), we have $y^* = \frac{\left(B^2-4A\right)(B+2)^2}{B^3(B+4)}$, i.e.,

$$\mathbf{E}_3^* = (x^*, y^*) = \left(-\frac{2}{B}, \frac{\left(B^2 - 4A\right)(B+2)^2}{B^3\,(B+4)}\right).$$

From all of the above, parameter B satisfies the following conditions:

$$\max\left\{-\frac{2}{E}, -2\sqrt{A}\right\} < B < -2, \quad 0 < -\frac{4\,(B+3)}{B\,(B+4)} < \frac{1}{2}.$$

Since,

$$y^* = \frac{\left(B^2 - 4A\right)(B+2)^2}{B^3\,(B+4)} > 0,$$

we finally get $B \in \left(\max\left\{-3, -2\sqrt{A}\right\}, 2\sqrt{3} - 6\right)$.
The following conclusion follows from the above.

Lemma 7. *Let $h > 0$, $C > 0$. If either*

$$6\left(2 - \sqrt{3}\right) < A < \frac{9}{4} \quad \textit{and} \quad -2\sqrt{A} < B < 2\sqrt{3} - 6,$$

or

$$A \geq \frac{9}{4} \quad \textit{and} \quad -3 < B < 2\sqrt{3} - 6,$$

and if

$$D = \frac{4C}{4A - B^2}, \quad E = -\frac{4\,(B+3)}{B\,(B+4)},$$

then the unique positive equilibrium point $\mathbf{E}_3^* = \left(-\frac{2}{B}, \frac{\left(B^2-4A\right)(B+2)^2}{B^3(B+4)}\right)$ is a 1:1 resonant fixed point of System (1.2).

Remark 8. *Y. Zeng and P. Yu [34] studied the continuous System (1.1). They established the existence of the extinction equilibrium ($\mathbf{E}_0 = (0,0)$), two boundary equilibria ($\mathbf{E}_1 = (E,0)$ and $\mathbf{E}_2 = (1,0)$), at most two interior equilibria ($\mathbf{E}_{3\pm}$), together with the corresponding existence conditions (Lemma 1). Using Lemma 1 and Theorem 2, they proved that the interior equilibrium undergoes codimension-1 bifurcations, including transcritical, saddle-node, and Hopf bifurcations. Furthermore, based solely on numerical simulations, they established the existence of a Bogdanov–Takens codimension-2 bifurcation point and provided the corresponding conditions, although no rigorous proof was provided.*

As we have already seen, the equilibrium states (equilibrium points) of System (1.2) are independent of the parameter $h > 0$. On the other hand, the dynamics of System (1.2) depend on the parameter h and are therefore richer than those of the corresponding continuous model (1.1). This is particularly evident at equilibrium $\boldsymbol{E}_2$, where an additional h-dependent bifurcation appears in the discrete case when $\lambda_1 = -1$ (a flip bifurcation), enabling the occurrence of a codimension-2 bifurcation (fold-flip) (near the point $\left(\widehat{h}, \widehat{D}\right)$ at the intersection of the bifurcation curves $h = \widehat{h}$ and $D = \widehat{D}$). We also established that the stability of the positive equilibrium $\boldsymbol{E}_{3+}$ depends on h. Furthermore, we observed that under certain conditions, the unique positive equilibrium $\left(-\frac{2}{B}, \overline{y}\right)$ is 1:1 resonant, a

property independent of h. However, when $h = 1$, the dynamics of the discrete system resemble those of the continuous model (at equilibrium $\boldsymbol{E}_2$, only a codimension-1 bifurcation—a transcritical bifurcation at $D = \widehat{D}$—occurs) and are less complex than the dynamics observed for arbitrary $h > 0$. We will restrict ourselves to the case where $h = 1$ to simplify the calculation process during the bifurcation analysis. This does not imply that the situation will remain unchanged for other values of the parameter h (for instance, it is unknown whether the non-degeneracy conditions for the equilibrium $\left(-\frac{2}{B}, \overline{y}\right)$ depend on h). However, due to their complexity and the extensive description required, we leave the investigation of these and other scenarios—specifically codimension-1 bifurcations and the aforementioned codimension-2 bifurcation at equilibrium $\boldsymbol{E}_2$—for future research.

4. Codimension-2 bifurcation at the interior equilibrium point

Since D and E are chosen as bifurcation parameters, in this section, we analyze the existence of a strong 1:1 bifurcation at the interior equilibrium point $\mathbf{E}_3^*$ by varying these parameters within a small neighborhood of (D^*, E^*). In doing so, we utilize the bifurcation theory established in [22, pp. 410–415].

All further considerations refer to the case where $h = 1$. Taking $D = D^*$ and $E = E^*$ in (3.4), we obtain

$$J_F\left(\mathbf{E}_3^*\right) = \begin{pmatrix} 1 & \frac{4}{B^2-4A} \\ 0 & 1 \end{pmatrix}.$$

Let

$$u_n = x_n - x^* = x_n + \frac{2}{B},$$
$$v_n = y_n - y^* = y_n - \frac{\left(B^2-4A\right)(B+2)^2}{B^3(B+4)},$$

and (α_1, α_2) denote a small perturbation of (D^*, E^*), i.e.,

$$\alpha_1 = E - E^*, \quad \alpha_2 = D - D^*.$$

Then, System (1.2) can be written in the form

$$\begin{cases} u_{n+1} = \frac{2}{B} + \left(u_n - \frac{2}{B}\right) P_1\left(\alpha_1\right) \\ v_{n+1} = -\frac{\left(B^2-4A\right)(B+2)^2}{B^3(B+4)} + \left(v_n + \frac{\left(B^2-4A\right)(B+2)^2}{B^3(B+4)}\right) P_2\left(\alpha_2\right), \end{cases} \tag{4.1}$$

where

$$P_1\left(\alpha_1\right) = e^{\left(1-u_n+\frac{2}{B}\right)\left(u_n-\frac{2}{B}-\alpha_1+\frac{4(B+3)}{B(B+4)}\right)-\frac{\left(u_n-\frac{2}{B}\right)\left(v_n+\frac{\left(B^2-4A\right)(B+2)^2}{B^3(B+4)}\right)}{A\left(u_n-\frac{2}{B}\right)^2+B\left(u_n-\frac{2}{B}\right)+1}},$$

$$P_2\left(\alpha_2\right) = e^{\frac{C\left(u_n-\frac{2}{B}\right)^2}{A\left(u_n-\frac{2}{B}\right)^2+B\left(u_n-\frac{2}{B}\right)+1}-\left(\alpha_2+\frac{4C}{4A-B^2}\right)}.$$

In doing so, $\mathbf{E}_3^* = (x^*, y^*)$ was transformed into the origin $(0, 0)$.

According to Taylor's formula to (4.1), around the origin $(u_n, v_n) = (0, 0)$, for any small $\|\boldsymbol{\alpha}\| = \|(\alpha_1, \alpha_2)\|$, we obtain

$$u_{n+1} = -\frac{2}{B}\left(e^{-\frac{B+2}{B}\alpha_1} - 1\right) + \left(1 - \frac{2}{B}\alpha_1\right) e^{-\frac{B+2}{B}\alpha_1} u_n - \frac{4}{4A-B^2} e^{-\frac{B+2}{B}\alpha_1} v_n$$

$$+\left(\alpha_1-\frac{\alpha_1^2}{B}+\frac{2\left(24A+2AB^2+12AB-8B^2-5B^3-B^4\right)}{B(B+4)\left(4A-B^2\right)}\right)e^{-\frac{B+2}{B}\alpha_1}u_n^2$$
$$-\frac{4}{4A-B^2}\alpha_1 e^{-\frac{B+2}{B}\alpha_1}u_nv_n-\frac{4B}{\left(4A-B^2\right)^2}e^{-\frac{B+2}{B}\alpha_1}v_n^2+O\left(\|(u_n,v_n)\|^3\right)$$

and

$$v_{n+1}=\frac{\left(4A-B^2\right)(B+2)^2}{B^3(B+4)}\left(1-e^{-\alpha_2}\right)+e^{-\alpha_2}v_n+\frac{BC(B+2)^2}{(B+4)\left(4A-B^2\right)}e^{-\alpha_2}u_n^2+O\left(\|(u_n,v_n)\|^3\right).$$

The map associated with the last two equations is given as

$$\begin{pmatrix}u\\v\end{pmatrix}\longmapsto f\left(u,v,\alpha_1,\alpha_2\right),\tag{4.2}$$

where f stands for the right-hand sides of the equations. The map (4.2) can be written in the following form:

$$\begin{pmatrix}u\\v\end{pmatrix}\longmapsto\begin{pmatrix}1&\frac{4}{B^2-4A}\\0&1\end{pmatrix}\begin{pmatrix}u\\v\end{pmatrix}+G\begin{pmatrix}u\\v\end{pmatrix},\tag{4.3}$$

where

$$G\begin{pmatrix}u\\v\end{pmatrix}=\begin{pmatrix}f_1(u,v)\\f_2(u,v)\end{pmatrix}$$

and

$$f_1(u,v)=-\frac{2}{B}\left(e^{-\frac{B+2}{B}\alpha_1}-1\right)+\left(\left(1-\frac{2}{B}\alpha_1\right)e^{-\frac{B+2}{B}\alpha_1}-1\right)u-\left(\frac{4}{4A-B^2}e^{-\frac{B+2}{B}\alpha_1}+\frac{4}{B^2-4A}\right)v-\frac{4\alpha_1}{4A-B^2}e^{-\frac{B+2}{B}\alpha_1}uv$$
$$+\left(\alpha_1-\frac{\alpha_1^2}{B}+\frac{2\left(24A+2AB^2+12AB-8B^2-5B^3-B^4\right)}{B(B+4)\left(4A-B^2\right)}\right)e^{-\frac{B+2}{B}\alpha_1}u^2-\frac{4B}{\left(4A-B^2\right)^2}e^{-\frac{B+2}{B}\alpha_1}v^2+O\left(\|(u,v)\|^3\right),$$

$$f_2(u,v)=\frac{\left(4A-B^2\right)(B+2)^2}{B^3(B+4)}\left(1-e^{-\alpha_2}\right)+\left(e^{-\alpha_2}-1\right)v+\frac{BC(B+2)^2}{(B+4)\left(4A-B^2\right)}e^{-\alpha_2}u^2+O\left(\|(u,v)\|^3\right).$$

Since 1 is a double eigenvalue of the matrix J_0, then there exist two real corresponding linearly independent vectors, $\widehat{v_0}$ (eigenvector) and $\widehat{v_1}$ (generalized eigenvector), such that

$$J_0\widehat{v_0}=\widehat{v_0}\quad\text{and}\quad J_0\widehat{v_1}=\widehat{v_1}+\widehat{v_0},$$

where

$$J_0=\begin{pmatrix}1&\frac{4}{B^2-4A}\\0&1\end{pmatrix}.$$

Without losing generality, we calculate $\widehat{v_0}$ as a unit vector, i.e., $\left\|\widehat{v_0}\right\|=1$, and then we obtain

$$\widehat{v_0}=\begin{pmatrix}1\\0\end{pmatrix}\quad\text{and}\quad\widehat{v_1}=\begin{pmatrix}0\\\frac{B^2-4A}{4}\end{pmatrix}.$$

Analogously, there exist corresponding adjoint eigenvectors,

$$\widehat{w_0} = \begin{pmatrix} 1 \\ 0 \end{pmatrix} \quad \text{and} \quad \widehat{w_1} = \begin{pmatrix} 0 \\ \frac{4}{B^2-4A} \end{pmatrix},$$

of transposed matrix J_0^T, given by

$$J_0^T w_1 = w_1 \quad \text{and} \quad J_0^T w_0 = w_0 + w_1,$$

such that $\left\|\widehat{v_0}\right\| = 1$. It can be shown that $\langle \widehat{v_0}, \widehat{w_0} \rangle = \langle \widehat{v_1}, \widehat{w_1} \rangle = 1$ and $\langle \widehat{v_0}, \widehat{w_1} \rangle = \langle \widehat{v_1}, \widehat{w_0} \rangle = 0$, where $\langle x, y \rangle$ denotes the standard scalar product of vectors x and y in $\mathbb{R}^2$.

Then, any vector $(u, v) \in \mathbb{R}^2$ can be uniquely represented as

$$\begin{aligned} \begin{pmatrix} u \\ v \end{pmatrix} &= m\widehat{v_0} + t\widehat{v_1} = m\begin{pmatrix} 1 \\ 0 \end{pmatrix} + t\begin{pmatrix} 0 \\ \frac{B^2-4A}{4} \end{pmatrix} \\ &= \begin{pmatrix} m \\ \left(\frac{B^2-4A}{4}\right)t \end{pmatrix} = \begin{pmatrix} 1 & 0 \\ 0 & \frac{B^2-4A}{4} \end{pmatrix}\begin{pmatrix} m \\ t \end{pmatrix}, \end{aligned}$$

where (m, t), as new coordinates, are qiven by

$$\begin{aligned} m &= \left\langle (u, v)^T, \widehat{w_0} \right\rangle = u, \\ t &= \left\langle (u, v)^T, \widehat{w_1} \right\rangle = \tfrac{4}{B^2-4A} v. \end{aligned}$$

By using these new coordinates, then (4.3) can be written in the form

$$\begin{pmatrix} 1 & 0 \\ 0 & \frac{B^2-4A}{4} \end{pmatrix}\begin{pmatrix} m \\ t \end{pmatrix} \to \begin{pmatrix} 1 & \frac{4}{B^2-4A} \\ 0 & 1 \end{pmatrix}\begin{pmatrix} 1 & 0 \\ 0 & \frac{B^2-4A}{4} \end{pmatrix}\begin{pmatrix} m \\ t \end{pmatrix} + \begin{pmatrix} f_1(m,t) + O\left(\|(m,t)\|^3\right) \\ f_2(m,t) + O\left(\|(m,t)\|^3\right) \end{pmatrix},$$

so by multiplying on the left side by the corresponding inverse matrix, we get

$$\begin{pmatrix} m \\ t \end{pmatrix} \to \begin{pmatrix} 1 & 1 \\ 0 & 1 \end{pmatrix}\begin{pmatrix} m \\ t \end{pmatrix} + \begin{pmatrix} 1 & 0 \\ 0 & -\frac{4}{4A-B^2} \end{pmatrix}\begin{pmatrix} f_1(m,t) + O\left(\|(m,t)\|^3\right) \\ f_2(m,t) + O\left(\|(m,t)\|^3\right) \end{pmatrix}.$$

Therefore, in the new coordinates (m, t), the map (4.3) takes the form

$$\begin{pmatrix} m \\ t \end{pmatrix} \longmapsto \begin{pmatrix} 1 & 1 \\ 0 & 1 \end{pmatrix}\begin{pmatrix} m \\ t \end{pmatrix} + \begin{pmatrix} \langle G(m\widehat{v_0} + t\widehat{v_1}), \widehat{w_0} \rangle + O\left(\|(m,t)\|^3\right) \\ \langle G(m\widehat{v_0} + t\widehat{v_1}), \widehat{w_1} \rangle + O\left(\|(m,t)\|^3\right) \end{pmatrix}, \tag{4.4}$$

where

$$G\begin{pmatrix} u \\ v \end{pmatrix} = \begin{pmatrix} f_1(u,v) \\ f_2(u,v) \end{pmatrix}.$$

Now, we have that

$$\widehat{f_1}(m, t, \alpha) = \langle G(m\widehat{v_0} + t\widehat{v_1}), \widehat{w_0} \rangle = \left\langle G\begin{pmatrix} m \\ \frac{B^2-4A}{4}t \end{pmatrix}, \begin{pmatrix} 1 \\ 0 \end{pmatrix} \right\rangle$$

$$= \left\langle \begin{pmatrix} f_1\left(m, \frac{B^2-4A}{4}t\right) \\ f_2\left(m, \frac{B^2-4A}{4}t\right) \end{pmatrix}, \begin{pmatrix} 1 \\ 0 \end{pmatrix} \right\rangle = f_1\left(m, \frac{B^2-4A}{4}t\right)$$

and

$$\begin{aligned} \widehat{f_2}(m,t,\boldsymbol{\alpha}) &= \langle G(s\widehat{v_0} + t\widehat{v_1}), \widehat{w_1}\rangle = \left\langle G\begin{pmatrix} m \\ \frac{B^2-4A}{4}t \end{pmatrix}, \begin{pmatrix} 0 \\ \frac{4}{B^2-4A} \end{pmatrix} \right\rangle \\ &= \left\langle \begin{pmatrix} f_1\left(m, \frac{B^2-4A}{4}t\right) \\ f_2\left(m, \frac{B^2-4A}{4}t\right) \end{pmatrix}, \begin{pmatrix} 0 \\ \frac{4}{B^2-4A} \end{pmatrix} \right\rangle = \frac{4}{B^2-4A} f_2\left(m, \frac{B^2-4A}{4}t\right), \end{aligned}$$

i.e.,

$$\begin{aligned} \widehat{f_1}(m,t,\boldsymbol{\alpha}) = &-\frac{2}{B}\left(e^{-\frac{B+2}{B}\alpha_1} - 1\right) + \left(e^{-\frac{B+2}{B}\alpha_1}\left(1 - \frac{2}{B}\alpha_1\right) - 1\right)m + \left(e^{-\frac{B+2}{B}\alpha_1} - 1\right)t + \alpha_1 e^{-\frac{B+2}{B}\alpha_1}mt \\ &- e^{-\frac{B+2}{B}\alpha_1}\left(\frac{1}{B}\alpha_1^2 - \alpha_1 + \frac{2\left(8B^2 - 2AB^2 - 12AB - 24A + 5B^3 + B^4\right)}{B\left(4A - B^2\right)(B+4)}\right)m^2 - \frac{B}{4}e^{-\frac{B+2}{B}\alpha_1}t^2 + O\left(\|(m,t)\|^3\right) \end{aligned}$$

and

$$\widehat{f_2}(m,t,\boldsymbol{\alpha}) = \frac{4(B+2)^2}{B^3(B+4)}\left(e^{-\alpha_2} - 1\right) + \left(e^{-\alpha_2} - 1\right)t - \frac{4BC(B+2)^2}{\left(4A - B^2\right)^2(B+4)}e^{-\alpha_2}m^2 + O\left(\|(m,t)\|^3\right).$$

If we introduce the notations for the coefficients of the polynomial in m and t as follows:

$$\begin{aligned} \widehat{f_1}(m,t,\boldsymbol{\alpha}) &= a_{00}(\boldsymbol{\alpha}) + a_{10}(\boldsymbol{\alpha})m + a_{01}(\boldsymbol{\alpha})t + \frac{1}{2}a_{20}(\boldsymbol{\alpha})m^2 + a_{11}(\boldsymbol{\alpha})mt + \frac{1}{2}a_{02}(\boldsymbol{\alpha})t^2, \\ \widehat{f_2}(m,t,\boldsymbol{\alpha}) &= b_{00}(\boldsymbol{\alpha}) + b_{10}(\boldsymbol{\alpha})m + b_{01}(\boldsymbol{\alpha})t + \frac{1}{2}b_{20}(\boldsymbol{\alpha})m^2 + b_{11}(\boldsymbol{\alpha})mt + \frac{1}{2}b_{02}(\boldsymbol{\alpha})t^2, \end{aligned}$$

from the above, we can notice that

$$\begin{aligned} a_{00}(\boldsymbol{\alpha}) &= -\frac{2}{B}\left(e^{-\frac{B+2}{B}\alpha_1} - 1\right), \\ b_{00}(\boldsymbol{\alpha}) &= \frac{4(B+2)^2}{B^3(B+4)}\left(e^{-\alpha_2} - 1\right), \\ a_{10}(\boldsymbol{\alpha}) &= e^{-\frac{B+2}{B}\alpha_1}\left(1 - \frac{2}{B}\alpha_1\right) - 1, \\ a_{01}(\boldsymbol{\alpha}) &= e^{-\frac{B+2}{B}\alpha_1} - 1, \\ b_{01}(\boldsymbol{\alpha}) &= e^{-\alpha_2} - 1, \\ a_{20}(\boldsymbol{\alpha}) &= \left(2\alpha_1 - \frac{2}{B}\alpha_1^2 - \frac{4\left(8B^2 - 2AB^2 - 12AB - 24A + 5B^3 + B^4\right)}{B\left(4A - B^2\right)(B+4)}\right)e^{-\frac{B+2}{B}\alpha_1}, \\ b_{20}(\boldsymbol{\alpha}) &= -\frac{8BC(B+2)^2}{\left(4A - B^2\right)^2(B+4)}e^{-\alpha_2}, \\ a_{11}(\boldsymbol{\alpha}) &= \alpha_1 e^{-\frac{B+2}{B}\alpha_1}, \end{aligned}$$

$$a_{02}(\boldsymbol{\alpha}) = -\frac{B}{2}e^{-\frac{B+2}{B}\alpha_1},$$
$$b_{10}(\boldsymbol{\alpha}) = 0, \quad b_{11}(\boldsymbol{\alpha}) = 0, \quad b_{02}(\boldsymbol{\alpha}) = 0.$$

In particular,

$$a_{00}(\mathbf{0}) = b_{00}(\mathbf{0}) = a_{10}(\mathbf{0}) = b_{10}(\mathbf{0}) = a_{01}(\mathbf{0}) = b_{01}(\mathbf{0}) = 0.$$

By using Lemma 9.6 in [22] or Lemma 3.1 in [33], for sufficiently small $\|\boldsymbol{\alpha}\|$, the map (4.4) can be written in the following form:

$$\begin{pmatrix} m \\ t \end{pmatrix} \longmapsto \Phi_{\boldsymbol{\alpha}}^{1}(m,t) + O\left(\|(m,t)\|^3\right),$$

where $\Phi_{\boldsymbol{\alpha}}^{1}(m,t)$ is the time-one flow of the following planar system:

$$\begin{pmatrix} m \\ t \end{pmatrix} \longmapsto \begin{pmatrix} 0 & 1 \\ 0 & 0 \end{pmatrix}\begin{pmatrix} m \\ t \end{pmatrix} + \begin{pmatrix} g_1(m,t,\boldsymbol{\alpha}) \\ g_2(m,t,\boldsymbol{\alpha}) \end{pmatrix}, \tag{4.5}$$

with

$$g_1(m,t,\boldsymbol{\alpha}) = A_{00}(\boldsymbol{\alpha}) + A_{10}(\boldsymbol{\alpha})m + A_{01}(\boldsymbol{\alpha})t + \frac{1}{2}A_{20}(\boldsymbol{\alpha})m^2 + A_{11}(\boldsymbol{\alpha})mt + \frac{1}{2}A_{02}(\boldsymbol{\alpha})t^2,$$
$$g_2(m,t,\boldsymbol{\alpha}) = B_{00}(\boldsymbol{\alpha}) + B_{10}(\boldsymbol{\alpha})m + B_{01}(\boldsymbol{\alpha})t + \frac{1}{2}B_{20}(\boldsymbol{\alpha})m^2 + B_{11}(\boldsymbol{\alpha})mt + \frac{1}{2}B_{02}(\boldsymbol{\alpha})t^2.$$

The appropriate coefficients $A_{00}(\boldsymbol{\alpha})$, $A_{10}(\boldsymbol{\alpha})$, $A_{01}(\boldsymbol{\alpha})$, $A_{20}(\boldsymbol{\alpha})$, $A_{11}(\boldsymbol{\alpha})$, $A_{02}(\boldsymbol{\alpha})$ and $B_{00}(\boldsymbol{\alpha})$, $B_{10}(\boldsymbol{\alpha})$, $B_{01}(\boldsymbol{\alpha})$, $B_{20}(\boldsymbol{\alpha})$, $B_{11}(\boldsymbol{\alpha})$, $B_{02}(\boldsymbol{\alpha})$ are given in Appendix A.

In particular, it is valid that

$$A_{00}(\mathbf{0}) = A_{10}(\mathbf{0}) = A_{01}(\mathbf{0}) = B_{00}(\mathbf{0}) = B_{10}(\mathbf{0}) = B_{01}(\mathbf{0}) = 0.$$

Moreover, equation (4.5) can be reduced to a simple system, i.e., the normal form of the Bogdanov–Takens bifurcation (Lemma 3.2 in [33], see Appendix B).

The first nondegeneracy condition

$$B_{20}(\mathbf{0}) = b_{20}(\mathbf{0}) = -\frac{8BC(B+2)^2}{(4A-B^2)^2(B+4)} \neq 0$$

holds due to the condition on the parameter B from Lemma 7.

Let

$$\Pi(A,B,C) = -2CB^2(B+2)^2 + \left(B^2\left(B^2+5B+8\right) - 2A\left(B^2+6B+12\right)\right)\left(4A-B^2\right).$$

The second nondegeneracy condition

$$A_{20}(\mathbf{0}) + B_{11}(\mathbf{0}) = -\frac{4\Pi(A,B,C)}{B(4A-B^2)^2(B+4)} \neq 0 \tag{4.6}$$

is satisfied if $\Pi(A,B,C) \neq 0$, i.e., if $C \neq C_s$, where

$$C_s = \frac{\left(4A - B^2\right)\left[B^2\left(B^2 + 5B + 8\right) - 2A\left(B^2 + 6B + 12\right)\right]}{2B^2(B+2)^2}. \tag{4.7}$$

Therefore

$$s = sgn\left[B_{20}(\mathbf{0})\left(A_{20}(\mathbf{0}) + B_{11}(\mathbf{0})\right)\right] = sgn\left[\Pi(A,B,C)\right].$$

If $C_s \leq 0$, then $\Pi(A,B,C) < 0$ for all C, i.e., $s = -1$. If $C_s > 0$, then $\Pi(A,B,C) < 0$ for $C > C_s$ and $\Pi(A,B,C) > 0$ for $C < C_s$. Therefore, both values for s, $s = -1$ and $s = 1$, are possible. For example, if $A = 2$ and $B = -\frac{27}{10}$ from (4.7), we get $C_s = \frac{163087}{2381400} > 0$, so

$$\Pi\left(2, -\frac{27}{10}, C_s\right) = 0$$

and

$$\begin{aligned} \Pi\left(2, -\tfrac{27}{10}, \tfrac{1}{100}\right) &= 0.41782 > 0, \\ \Pi\left(2, -\frac{27}{10}, \frac{1}{2}\right) &= -3.0828 < 0, \end{aligned} \tag{4.8}$$

where $\frac{1}{100} < C_s < \frac{1}{2}$.

By using (4.6), we get

$$\beta_0(\mathbf{0}) = \frac{-4\Pi(A,B,C)}{B\left(4A - B^2\right)^2(B+4)},$$

so

$$\begin{cases} \eta_1(\boldsymbol{\alpha}) = -\dfrac{4\left[\Pi(A,B,C)\right]^4}{B^7C^3\left(4A - B^2\right)^2(B+2)^6(B+4)}\beta_1(\boldsymbol{\alpha}) \\ \qquad\qquad - \dfrac{\left[\Pi(A,B,C)\right]^3}{B^6C^3(B+2)^6}\beta_2(\boldsymbol{\alpha})\beta_3(\boldsymbol{\alpha}) + \dfrac{\left[\Pi(A,B,C)\right]^2}{B^4C^2(B+2)^4}\beta_2^2(\boldsymbol{\alpha}), \\ \eta_2(\boldsymbol{\alpha}) = \dfrac{\left[\Pi(A,B,C)\right]^2}{B^4C^2(B+2)^4}\beta_4(\boldsymbol{\alpha}) - \dfrac{2\Pi(A,B,C)}{B^2C(B+2)^2}\beta_2(\boldsymbol{\alpha}), \end{cases} \tag{4.9}$$

where

$$\begin{aligned} \beta_1(\boldsymbol{\alpha}) = {} & \frac{4(B+2)^2}{B^3(B+4)}\left(\frac{1}{B}\alpha_1 e^{-\frac{B+2}{B}\alpha_1} + 1\right)\left(e^{-\alpha_2} - 1\right) \\ & - \frac{8C(B+2)^2}{3B\left(4A - B^2\right)^2(B+4)}\left(e^{-\frac{B+2}{B}\alpha_1} - 1\right)^2 - \frac{2(B+2)^2\left(B^3 + 6B^2 + 8B + 8\right)}{B^5(B+4)^2}\left(e^{-\alpha_2} - 1\right)^2 \\ & + \frac{16(B+2)^4\left(\frac{24A + 2AB^2 + 12AB - 8B^2 - 5B^3 - B^4}{3B^2\left(4A - B^2\right)} + \frac{C(B+2)^2}{2\left(4A - B^2\right)^2}\right)}{B^5(B+4)^3}\left(e^{-\alpha_2} - 1\right)^2 \\ & + \frac{16(B+2)^2\left(\frac{24A + 2AB^2 + 12AB - 8B^2 - 5B^3 - B^4}{B^2\left(4A - B^2\right)} + \frac{C(B+2)^2}{\left(4A - B^2\right)^2}\right)}{3B^3(B+4)^2}\left(e^{-\frac{B+2}{B}\alpha_1} - 1\right)\left(e^{-\alpha_2} - 1\right) \end{aligned}$$

$$+\frac{2\left(B^3+3B^2-4B-4\right)}{B^3(B+4)}\left(e^{-\frac{B+2}{B}\alpha_1}-1\right)\left(e^{-\alpha_2}-1\right),$$

$$\begin{aligned}\beta_2(\boldsymbol{\alpha}) &= -\frac{2}{B}\alpha_1 e^{-\frac{B+2}{B}\alpha_1}+e^{-\frac{B+2}{B}\alpha_1}-1+\frac{\left(B^3+2B^2-8B-8\right)}{B^2(B+4)}\left(e^{-\alpha_2}-1\right)\\ &\quad-\frac{4}{B+4}\left(\frac{24A+2AB^2+12AB-8B^2-5B^3-B^4}{B^2(4A-B^2)}+\frac{2C(B+2)^2}{(4A-B^2)^2}\right)\left(e^{-\frac{B+2}{B}\alpha_1}-1\right)\\ &\quad-\frac{4(B+2)^2}{3B^2(B+4)^2}\left(\frac{24A+2AB^2+12AB-8B^2-5B^3-B^4}{B^2(4A-B^2)}+\frac{2C(B+2)^2}{(4A-B^2)^2}\right)\left(e^{-\alpha_2}-1\right),\end{aligned}$$

$$\begin{aligned}\beta_3(\boldsymbol{\alpha}) &= \frac{8C(B+2)^2}{(4A-B^2)^2(B+4)}\left(e^{-\frac{B+2}{B}\alpha_1}-1\right)\\ &\quad-\frac{8(B+2)^2}{B^3(B+4)}\left(\frac{24A+2AB^2+12AB-8B^2-5B^3-B^4}{B(4A-B^2)(B+4)}+\frac{BC(B+2)^2}{3(4A-B^2)^2(B+4)}\right)\left(e^{-\alpha_2}-1\right),\end{aligned}$$

$$\begin{aligned}\beta_4(\boldsymbol{\alpha}) &= \frac{8C(B+2)^2}{(4A-B^2)^2(B+4)}\left(e^{-\frac{B+2}{B}\alpha_1}-1\right)\\ &\quad+\frac{8(B+2)^2}{B^3(B+4)}\left(\frac{24A+2AB^2+12AB-8B^2-5B^3-B^4}{B(4A-B^2)(B+4)}+\frac{3BC(B+2)^2}{(4A-B^2)^2(B+4)}\right)\left(e^{-\alpha_2}-1\right).\end{aligned}$$

Then,

$$\frac{\partial(\eta_1(\mathbf{0}))}{\partial\alpha_1}=0,$$

$$\frac{\partial(\eta_1(\mathbf{0}))}{\partial\alpha_2}=\frac{16[\Pi(A,B,C)]^4}{B^{10}C^3(4A-B^2)^2(B+4)^2(B+2)^4},$$

$$\frac{\partial(\eta_2(\mathbf{0}))}{\partial\alpha_1}=\frac{2(B+4)\Pi(A,B,C)}{B^3C(B+2)^2},$$

which implies that

$$\begin{aligned}\det J_{\alpha}\boldsymbol{\eta}(\mathbf{0}) &= \det\begin{bmatrix}0 & \frac{\partial(\eta_1(\mathbf{0}))}{\partial\alpha_2}\\ \frac{\partial(\eta_2(\mathbf{0}))}{\partial\alpha_1} & \frac{\partial(\eta_2(\mathbf{0}))}{\partial\alpha_2}\end{bmatrix}=-\frac{\partial(\eta_1(\mathbf{0}))}{\partial\alpha_2}\cdot\frac{\partial(\eta_2(\mathbf{0}))}{\partial\alpha_1}\\ &=-\frac{32[\Pi(A,B,C)]^5}{B^{13}C^4(4A-B^2)^2(B+2)^6(B+4)}.\end{aligned}$$

According to the transversality condition, we have that

$$\det J_{\alpha}\boldsymbol{\eta}(\mathbf{0})\neq 0\Leftrightarrow\Pi(A,B,C)\neq 0\Leftrightarrow C\neq C_s.$$

Hence, both the nondegeneracy and transversality conditions are given by $C\neq C_s$.

Therefore, according to [22, pp. 410–415], the following results hold.

Theorem 9. *Let $h = 1$, $C > 0$, $D > 0$, $0 < E < 1/2$,*

$$D^* = \frac{4C}{4A - B^2}, \quad E^* = -\frac{4(B+3)}{B(B+4)},$$

$$C_s = \frac{\left(4A - B^2\right)\left[B^2\left(B^2 + 5B + 8\right) - 2A\left(B^2 + 6B + 12\right)\right]}{2B^2(B+2)^2}.$$

Assume that either

$$6\left(2 - \sqrt{3}\right) < A < \frac{9}{4} \quad \text{and} \quad -2\sqrt{A} < B < 2\sqrt{3} - 6,$$

or

$$A \geq \frac{9}{4} \quad \text{and} \quad -3 < B < 2\sqrt{3} - 6.$$

If $C \neq C_s$, then System (1.2) undergoes a Bogdanov–Takens bifurcation in a small neighborhood of the unique interior fixed point

$$\boldsymbol{E}_3^* = \left(-\frac{2}{B}, \frac{\left(B^2 - 4A\right)(B+2)^2}{B^3(B+4)}\right)$$

as (E, D) varies near (E^*, D^*).
Furthermore, the following statements hold:

(i) *There is a fold bifurcation that occurs on the curve*

$$f_{\pm} : \eta_1(\alpha) = \frac{1}{4}\eta_2^2(\alpha) + O\left(|\alpha|^3\right).$$

(ii) *Near the fixed point born at the fold bifurcation of (i), there is a Neimark–Sacker bifurcation that occurs on the curve*

$$NS : \eta_1(\alpha) = O\left(|\alpha|^3\right), \ \eta_2(\alpha) = O\left(|\alpha|^2\right) < 0.$$

If $C_s \leqslant 0$ or $0 < C_s < C$, the invariant circle created at the Neimark–Sacker bifurcation is stable. If $C < C_s$, the invariant circle created at the Neimark–Sacker bifurcation is unstable.

(iii) *There is a homoclinic bifurcation that occurs on two curves h_1 and h_2 with the asymptotic forms*

$$\eta_1(\alpha) = -\frac{6}{25}\eta_2^2(\alpha) + O\left(|\alpha|^3\right), \ \eta_2(\alpha) = O\left(|\alpha|^2\right) < 0,$$

where η_1 and η_2 are given by (4.9). The distance between the two homoclinic tangency bifurcation curves is exponentially small with respect to $\sqrt{|\alpha|}$. These curves are illustrated in Figure 1 in [27].

5. Numerical simulations

This section illustrates the complex dynamics of 1:1 resonance through carefully designed numerical simulations. Bifurcation diagrams and phases portraits in all figures are generated by Dynamica 4 [19].

Case $s = -1$.

Let $A = \frac{1529}{400}, B = -\frac{27}{10}$, and $C = 2$. The straightforward calculation shows that

$$B_{20}(\mathbf{0}) = b_{20}(\mathbf{0}) = \frac{1323}{5200} \neq 0$$

and

$$\Pi(A, B, C) = F\left(\frac{1529}{400}, -\frac{27}{10}, 2\right) = -\frac{2472}{25},$$

so $s = -1$. Figure 1 (as well as Figure 8.8 in [22, p. 322]) illustrates the bifurcation diagram of the system in Lemma 11 in the (η_1, η_2) plane, where the coordinates (4.9) are introduced through the transformation

$$\begin{aligned}
\eta_1(\boldsymbol{\alpha}) = {} & \frac{10863616000000}{103355177121}\alpha_1^2 e^{-\frac{14}{27}\alpha_1} + \frac{91866722756710400000}{343803451765076667}\alpha_1 e^{-\alpha_2} e^{-\frac{7}{27}\alpha_1} \\
& + \frac{1086361600000}{3827969523}\alpha_1 e^{-\frac{14}{27}\alpha_1} - \frac{189436691822796800000}{343803451765076667}\alpha_1 e^{-\frac{7}{27}\alpha_1} \\
& + \frac{697830973406720000}{4244487058828107}e^{-\frac{14}{27}\alpha_1} + \frac{189279426636668142401766400000}{92634603856208443256483529}e^{-2\alpha_2} \\
& + \frac{1044217022081434575072818176000}{45390955889542137195676929 21}e^{-\alpha_2} - \frac{14688378654754419114342400 00}{47895912091951184125437 3}e^{-\alpha_2} e^{-\frac{7}{27}\alpha_1} \\
& + \frac{1311347688245135701166080000}{47895912091951184125437 3}e^{-\frac{7}{27}\alpha_1} - \frac{10623372206528213671141160960000}{45390955889542137195676929 21},
\end{aligned}$$

$$\eta_2(\boldsymbol{\alpha}) = \frac{3322702342614400}{86622184874043}e^{-\alpha_2} + \frac{329600}{11907}e^{-\frac{7}{27}\alpha_1} + \frac{6592000}{321489}\alpha_1 e^{-\frac{7}{27}\alpha_1} - \frac{5720508014444800}{86622184874043}.$$

For $E = \alpha_1 - \frac{4(B+3)}{B(B+4)}$ and $D = \alpha_2 + \frac{4C}{4A-B^2}$, System (1.2) becomes

$$\begin{cases} x_{n+1} = x_n e^{(1-x_n)\left(x-\alpha_1+\frac{4(B+3)}{B(B+4)}\right)-\frac{x_n y_n}{Ax_n^2+Bx_n+1}}, \\ y_{n+1} = y_n e^{\frac{Cx_n^2}{Ax_n^2+Bx_n+1}-\alpha_2-\frac{4C}{4A-B^2}}. \end{cases} \tag{5.1}$$

Also, for the given parameters, the equilibrium points of System (5.1) satisfy the following system:

$$\begin{cases} \overline{x}_{\pm} = \frac{540(\alpha_2+1)\pm 400K}{1529\alpha_2+729}, \\ \overline{y}_{\pm} = \frac{40(7(\alpha_2+1)\mp 20K)(71\alpha_2-729\mp 1080K)P_y}{117(\alpha_2+1)(1529\alpha_2+729)^3}, \end{cases}$$

where

$$P_y = (85293\alpha_1 - 2020\alpha_2 + 178893\alpha_1\alpha_2 - 34020 \mp 46800K).$$

So, for $\alpha_2 \neq -\frac{729}{1529}$ and $K = \sqrt{-2\alpha_2(\alpha_2+1)}$, we have $(\overline{x}, \overline{y}) = (\overline{x}_{\pm}, \overline{y}_{\pm})$ with

$$\begin{cases} \overline{y} = \frac{\overline{x}-1}{\overline{x}}\left(\frac{1529}{400}\overline{x}^2 - \frac{27}{10}\overline{x} + 1\right)\left(-\overline{x} + \alpha_1 + \frac{40}{117}\right), \\ \overline{x}^2(1529\alpha_2 + 729) - 1080\overline{x}(\alpha_2+1) + 400(\alpha_2+1) = 0. \end{cases} \tag{5.2}$$

For $(\alpha_1, \alpha_2) = (0, 0)$, we have point $O = O(\eta_1(0,0), \eta_2(0,0)) = (0,0)$ and the 1:1 resonant fixed point $(x^*, y^*) = (\frac{20}{27}, \frac{39200}{255879})$ or

$$(x^*, y^*) = (0.7407407407407407, 0.15319740971318474),$$

corresponding to a codimension-2 cusp. The blue curve and red lines in Figures 2–9 represent the first and second equations of system (5.2), respectively, in the Cartesian coordinate plane. When it exists, the positive equilibrium of System (4.1) is given by the intersection of these curves. Figure 2 displays the phase portrait at point O in the (η_1, η_2) plane (see Figure 1). The equilibrium point of System (5.1) is at the intersection of the red and blue curves.

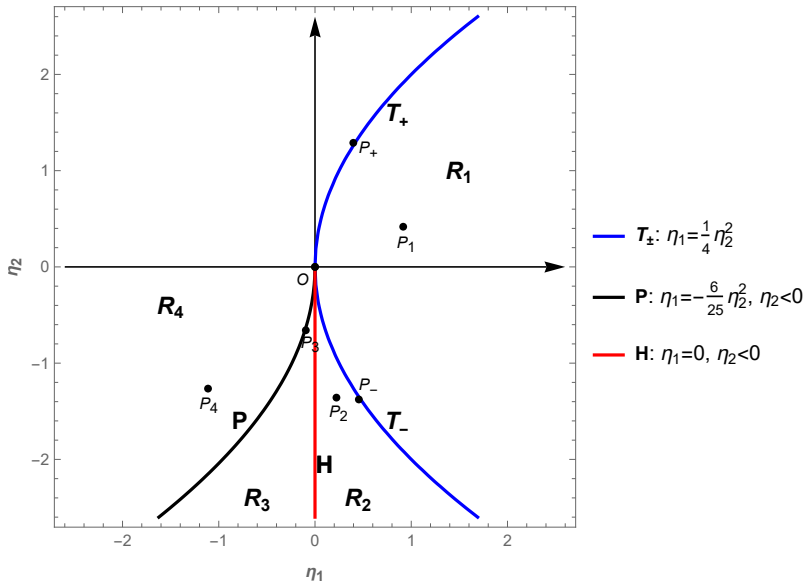


Figure 1. The bifurcation diagram of the system in Lemma 11 in the $\eta_1\eta_2$-plane.

In Table 3, coordinates η_1 and η_2 are calculated as $\eta_1 = \eta_1(\alpha_1, \alpha_2)$ and $\eta_2 = \eta_2(\alpha_1, \alpha_2)$, respectively, while points $P_1(\eta_1, \eta_2)$–$P_4(\eta_1, \eta_2)$ and $P_\pm(\eta_1, \eta_2)$ belong to the corresponding region in Figure 1.

To construct Figures 3–6, we use the parameter values from Table 3 for small α_1 and α_2.
Figure 3(a) displays the phase portrait at point $P_1(\eta_1, \eta_2) \in \mathbf{R_1}$, when there is no positive equilibrium point of System (5.1). Figure 3(b) displays the phase portrait at point $P_2(\eta_1, \eta_2) \in \mathbf{R_2}$. The positive equilibria of System (5.1) are

$$(\overline{x}_+, \overline{y}_+) = (0.723782419330519, 0.19278149447692491),$$

$$(\overline{x}_-, \overline{y}_-) = (0.7585127997297987, 0.189358984144891).$$

Figure 4(a) ilustrates the phase portret of System (5.1) at $P_3 \in \mathbf{R_3}$. The positive equilibria of System (5.1) are

$$(\overline{x}_+, \overline{y}_+) = (0.723782419330519, 0.17277935052509102),$$

$$(\overline{x}_-, \overline{y}_-) = (0.7585127997297987, 0.171032707769117).$$

Around the positive equilibrium $(\overline{x}_+, \overline{y}_+)$, there is stable invariant curve.
Figure 4(b) is an enlargement of Figure 4(a) with a boundary equilibrium.

Figure 5 ilustrates the phase portrait of System (5.1) at $P_4 \in \mathbf{R_4}$. The positive equilibria of System (5.1) are

$$(\overline{x}_+, \overline{y}_+) = (0.6981468468399172, 0.19346498347102042),$$

$$(\overline{x}_-, \overline{y}_-) = (0.7888696254901314, 0.1832259851917776).$$

Figure 6(a) presents phase portraits of System (5.1) at $P_- \in \mathbf{T}_-$. The positive equilibrium of System (5.1) is $(x^{\pm}, y^{\pm}) = (\frac{20}{27}, \frac{49028}{255879})$ or

$$(\overline{x}_{\pm}, \overline{y}_{\pm}) = (0.7407407407407407, 0.19160618886270464)$$

(see the small illustration for T_- in Figure 8.8 [22, p. 322]).

Figure 6(b) presents phase portraits of System (5.1) at $P_+ \in \mathbf{T_+}$. The positive equilibrium of System (5.1) is $(x^{\pm}, y^{\pm}) = (\frac{20}{27}, \frac{29372}{255879})$ or

$$(\overline{x}_{\pm}, \overline{y}_{\pm}) = (0.7407407407407407, 0.11478863056366485)$$

(see the small illustration for T_+ in Figure 8.8 [22, p. 322]).

(α_1,α_2)	(η_1, η_2)	Reg.	Fig.
$(0.039578, 0.0026951)$	$P_1 = (0.91639, 0.41742)$	$\mathbf{R}_1$	3(a)
$(-0.1, -0.0005)$	$P_2 = (0.22271, -1.3581)$	$\mathbf{R}_2$	3(b)
$(-0.05, -0.0005)$	$P_3 = (-0.095453, -0.65826)$	$\mathbf{R}_3$	4
$(-0.1012, -0.0033804)$	$P_4 = (-1.1116, -1.2645)$	$\mathbf{R}_4$	5
$(-0.1, 0.0)$	$P_- = (0.45549, -1.3773)$	$\mathbf{T}_-$	6(a)
$(0.01, 0.0)$	$P_+ = (0.39795, 1.2895)$	$\mathbf{T}_+$	6(b)

Table 3. Description of the values (α_1,α_2) for which simulations were made in Figures 3–6.

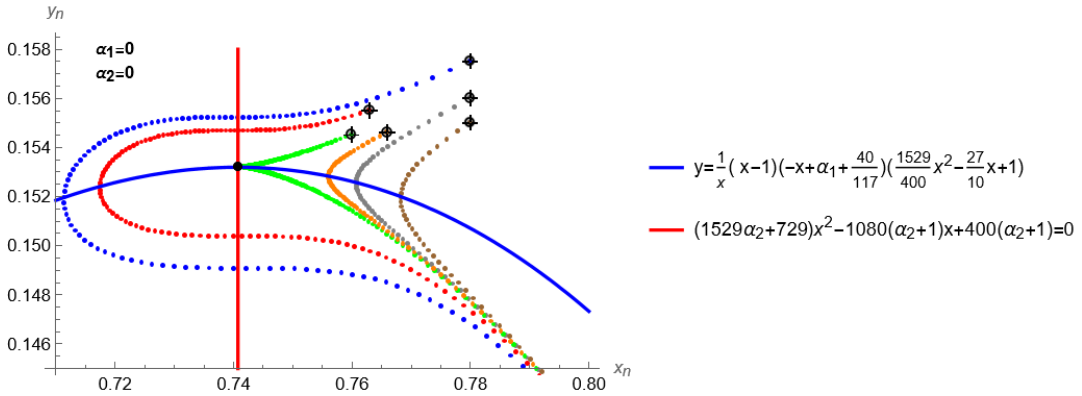
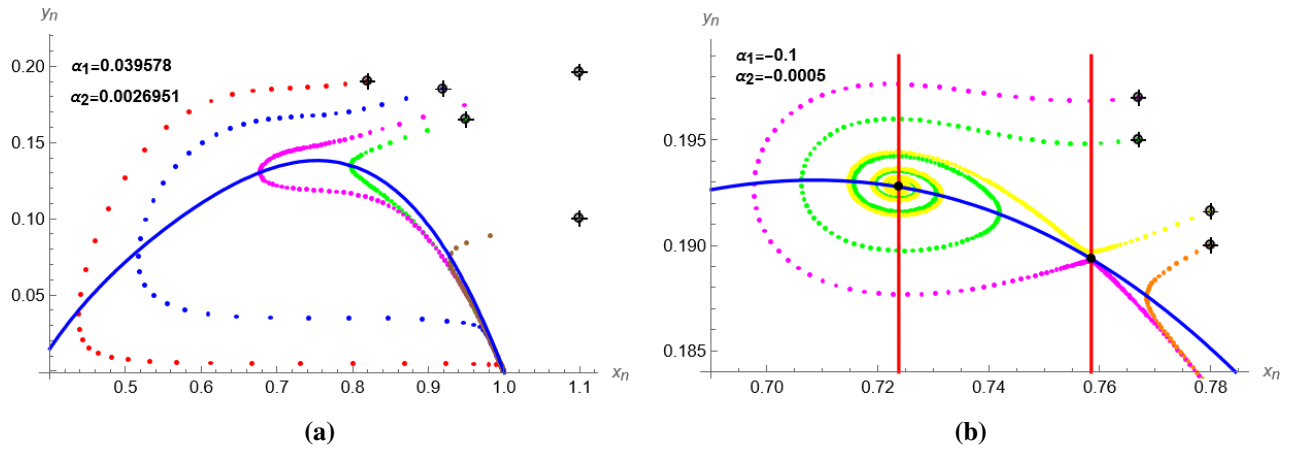
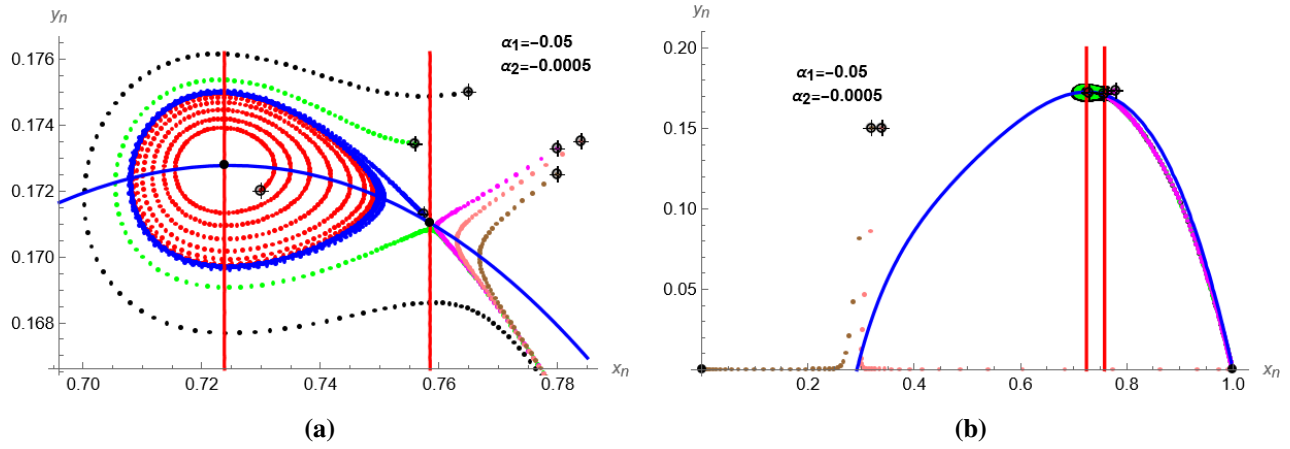


Figure 2. Phase portraits of System (5.1) at $O(\eta_1, \eta_2) = (0, 0)$.



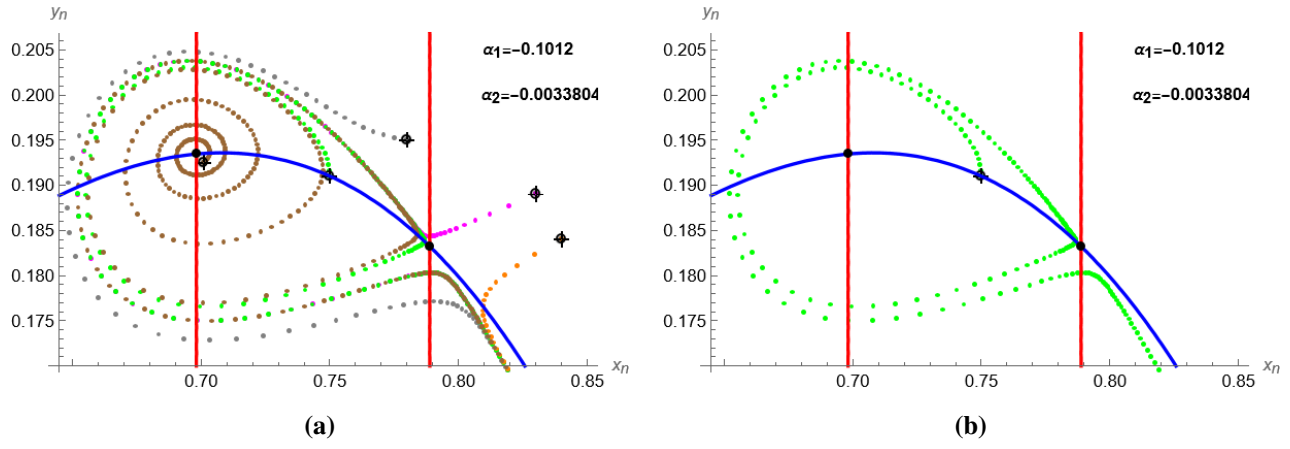
(a) **(b)**

Figure 3. Phase portraits of System (5.1): (a) $P_1(\eta_1, \eta_2) \in \mathbf{R_1}$, (b) $P_2(\eta_1, \eta_2) \in \mathbf{R_2}$.



(a) **(b)**

Figure 4. Phase portraits of System (5.1) at $P_3(\eta_1, \eta_2) \in \mathbf{R_3}$.



(a) **(b)**

Figure 5. Phase portraits of System (5.1) at $P_4(\eta_1, \eta_2) \in \mathbf{R_4}$.

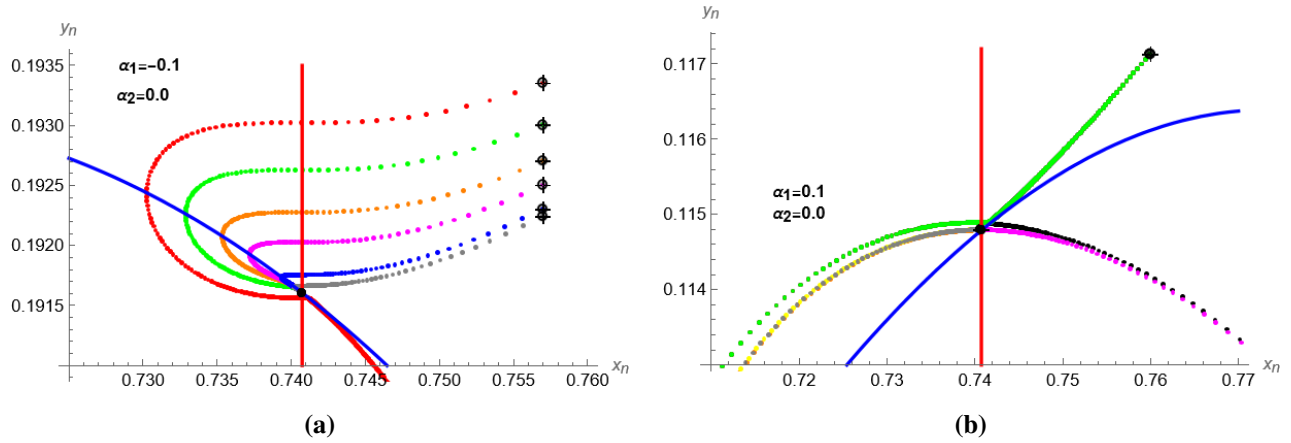


Figure 6. Phase portraits of System (5.1) at: (a) $P_{-}(\eta_1, \eta_2) \in \mathbf{T}_{-}$, (b) $P_{+}(\eta_1, \eta_2) \in \mathbf{T}_{+}$.

Figures 2–9 show 1500 iterations of the corresponding orbits. In Figure 2, the orbits are depicted in gray, red, green, orange, blue, and brown, corresponding to the initial conditions $(0.78, 0.156)$, $(0.763, 0.1555)$, $(0.75995, 0.15451)$, $(0.766, 0.1546)$, $(0.78, 0.1575)$, and $(0.78, 0.155)$, respectively. In Figure 3(a), the orbits are depicted in green, magenta, blue, red, and brown, corresponding to the initial conditions $(0.95, 0.165)$, $(1.19, 0.196)$, $(0.92, 0.185)$, $(0.82, 0.19)$, and $(1.195, 0.1)$, respectively. In Figure 3(b), the orbits are depicted in green, magenta, orange, and yellow, corresponding to the initial conditions $(0.767, 0.195)$, $(0.767, 0.197)$, $(0.78, 0.19)$, and $(0.78, 0.1916)$, respectively. In Figure 4(a), the orbits are depicted in red, blue, black, green, magenta, pink, and brown, corresponding to the initial conditions $(0.73, 0.172)$, $(0.7575, 0.1713)$, $(0.765, 0.175)$, $(0.756, 0.17343)$, $(0.78, 0.17328)$, $(0.784, 0.1735)$, and $(0.78, 0.1725)$, respectively. In Figure 4(b), the orbits are depicted in red, blue, black, green, magenta, pink, and brown, corresponding to the initial conditions $(0.73, 0.172)$, $(0.7575, 0.1713)$, $(0.765, 0.175)$, $(0.756, 0.17343)$, $(0.78, 0.17328)$, $(0.34, 0.15)$, and $(0.32, 0.15)$, respectively. In Figure 5(a), the orbits are depicted in magenta, green, orange, gray, and brown, corresponding to the initial conditions $(0.83, 0.189)$, $(0.75, 0.191)$, $(0.84, 0.184)$, $(0.78, 0.195)$, and $(0.701, 0.1925)$, respectively. In Figure 5(b), the orbit is depicted in green, with the initial condition $(0.75, 0.191)$. In Figure 6(a), the orbits are depicted in red, green, black, orange, magenta, blue, and gray, corresponding to the initial conditions $(0.757, 0.1937)$, $(0.757, 0.193)$, $(0.757, 0.195)$, $(0.757, 0.191)$, $(0.757, 0.1925)$, $(0.757, 0.1923)$, and $(0.757, 0.19205)$, respectively. In Figure 6(b), the orbits are depicted in black, orange, magenta, and green, corresponding to the initial conditions $(0.76, 0.11712511037004324)$, $(0.74070, 0.114785)$, $(0.740746, 0.114789)$, and $(0.76, 0.11712511037004375)$, respectively.

Case $s = 1$.

Let $A = 2$, $B = -\frac{27}{10}$, and $C = \frac{1}{100}$. From (4.8), we have $s = 1$.

Figure 7, similar to the case of $s = -1$, shows the phase portrait of System (5.1) at the 1:1 resonant fixed point $(x^*, y^*) = (\frac{20}{27}, \frac{3479}{255879})$ or

$$(x^*, y^*) = (0.7407407407407407, 0.013596270112045146),$$

which has a cusp of codimension-2.

Figures 8–9 show the phase portraits of System (5.1) for small α_1 and α_2 from Table 4. The bifurcation diagram and the regions R_1, R_2, R_3, and R_4 are the same as in the case of $s = -1$ in Figure 1.

Indeed, in the case when $s = 1$, we introduce the substitutions

$$t = -\tau, \quad v_1 = u_1, \quad v_2 = -u_2.$$

Then,

$$\dot{v}_1 = \frac{dv_1}{dt} \overset{t=-\tau}{=} -\frac{dv_1}{d\tau} \overset{v_1=u_1}{=} -\frac{du_1}{d\tau} = -u_1',$$

so, for $s = 1$, the first equation of the system in Lemma 11 becomes

$$\dot{v}_1 = v_2 \Longleftrightarrow -u_1' = -u_2 \Longleftrightarrow u_1' = u_2.$$

Furthermore, we have

$$\dot{v}_2 = \frac{dv_2}{dt} \overset{t=-\tau}{=} -\frac{dv_2}{d\tau} \overset{v_2=-u_2}{=} -\frac{d(-u_2)}{d\tau} = u_2',$$

so, for $s = 1$, the second equation of the system in Lemma 11 becomes

$$\begin{aligned} \dot{v}_2 &= \eta_1(\alpha) + \eta_2(\alpha) v_1 + v_1^2 + v_1 v_2 \\ &\Longleftrightarrow u_2' = \eta_1(\alpha) + \eta_2(\alpha) u_1 + u_1^2 + u_1(-u_2) \\ &\Longleftrightarrow u_2' = \eta_1(\alpha) + \eta_2(\alpha) u_1 + u_1^2 - u_1 u_2. \end{aligned}$$

Therefore, similarly to the case where $s = -1$, the parametric portrait remains unchanged; however, the curve loses stability in the vicinity of the Bogdanov–Takens point. A stable curve is shown in Figure 4, whereas an unstable curve is depicted in Figure 9.

(α_1, α_2)	(η_1, η_2)	Reg.	Fig.
$(0.01, 0.006)$	$Q_1 = (0.67556, 0.041124)$	$\mathbf{R}_1$	8(a)
$(0.054888, -0.0024273)$	$Q_4 = (-0.14149, -0.669466)$	$\mathbf{R}_4$	8(b)
$(0.04322, -0.00078251)$	$Q_3 = (-0.02, -0.5)$	$\mathbf{R}_3$	9

Table 4. Description of the values for which simulations were made in Figures 8–9.

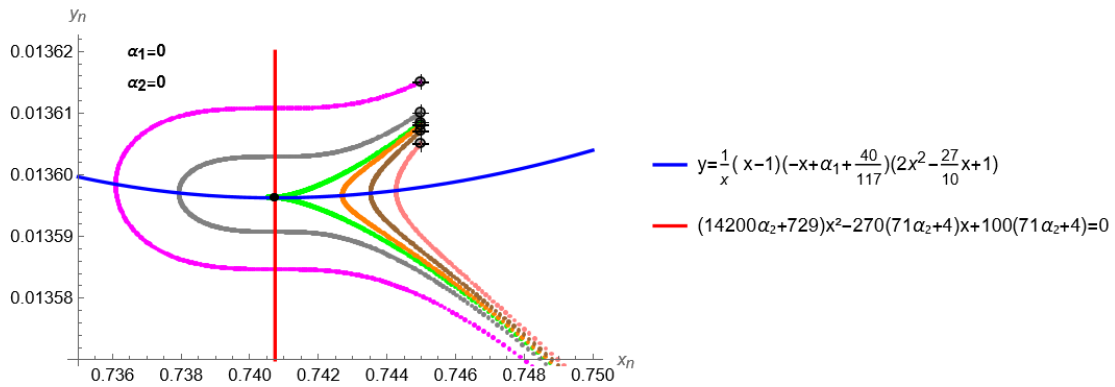


Figure 7. Phase portraits of System (5.1) at $O(\eta_1, \eta_2) = (0, 0)$.

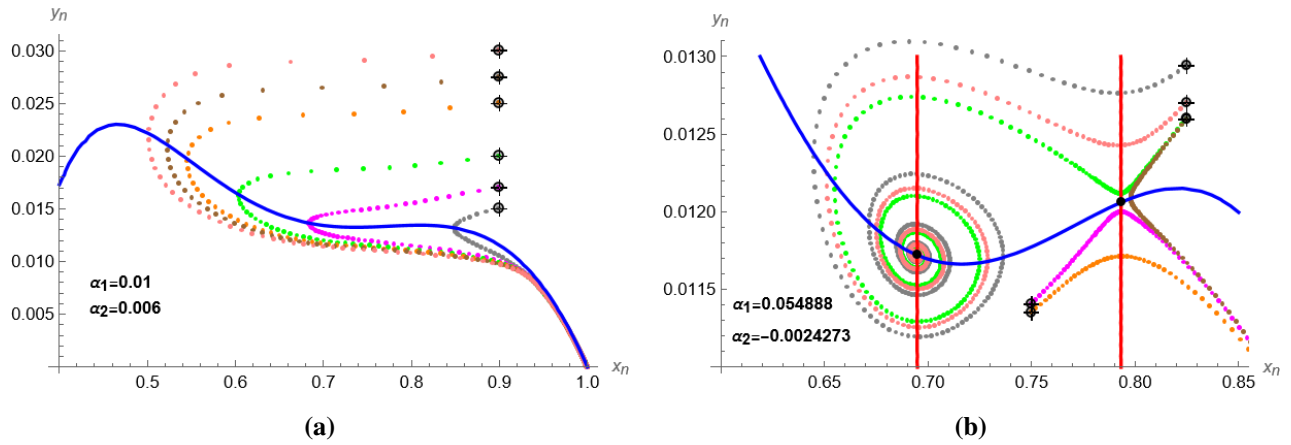


Figure 8. Phase portraits of System (5.1) at: (a) $Q_1(\eta_1, \eta_2) \in \mathbf{R_1}$, (b) $Q_4(\eta_1, \eta_2) \in \mathbf{R_4}$.

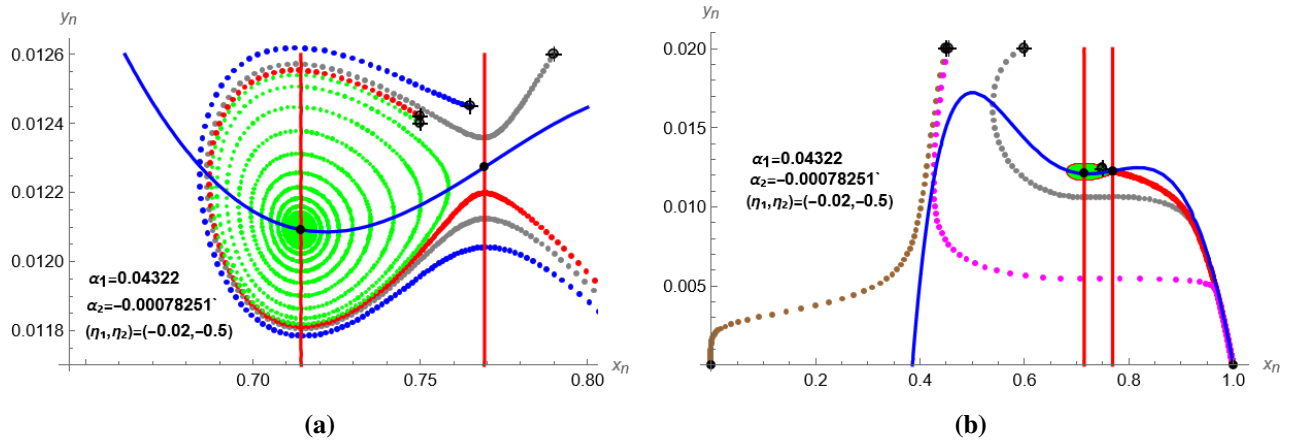


Figure 9. Phase portraits of System (5.1) at $Q_3(\eta_1, \eta_2) \in \mathbf{R_3}$.

In Figure 7, the orbits are depicted in gray, magenta, green, orange, brown, and pink, corresponding to the initial conditions $(0.745, 0.01361)$, $(0.745, 0.013615)$, $(0.745, 0.0136084635)$, $(0.745, 0.013608)$, $(0.745, 0.013607)$, and $(0.745, 0.013605)$, respectively. In Figure 8(a), the orbits are depicted in gray, magenta, green, orange, brown, and pink, corresponding to the initial conditions $(0.9, 0.015)$, $(0.9, 0.017)$, $(0.9, 0.02)$, $(0.9, 0.025)$, $(0.9, 0.0275)$, and $(0.9, 0.03)$, respectively. In Figure 8(b), the orbits are depicted in gray, magenta, green, orange, brown, and pink, corresponding to the initial conditions $(0.825, 0.01294)$, $(0.75, 0.011404)$, $(0.825, 0.012599)$, $(0.75, 0.01135)$, $(0.825, 0.012595)$, and $(0.825, 0.0127)$, respectively. In Figure 9(a), the orbits are depicted in gray, blue, red, and green, corresponding to the initial conditions $(0.79, 0.0126)$, $(0.765, 0.01245)$, $(0.75, 0.01242)$, and $(0.75, 0.0124)$, respectively. In Figure 9(b), the orbits are depicted in gray, brown, red, green, and magenta, corresponding to the initial conditions $(0.6, 0.02)$, $(0.45, 0.02)$, $(0.75, 0.01242)$, $(0.75, 0.0124)$, and $(0.455, 0.02)$, respectively.

Remark 10. *We note that, from the above discussion, Figures 2–9 show phase portraits obtained by visualizations and numerical calculations for specific situations (with concrete equilibrium points and*

parameter values), as illustrated in Figure 8.8 in [22, p. 322].

6. Conclusions

This paper provides a discrete counterpart to the analysis of the corresponding continuous system in [34], where only codimension-1 bifurcations were considered, while the numerical illustrations suggested the possible occurrence of a codimension-2 Bogdanov–Takens bifurcation. Motivated by this, we conducted a detailed study of the bifurcation. Using normal form theory, we derived explicit parameter conditions ensuring the existence of a positive equilibrium exhibiting the Bogdanov–Takens singularity. Furthermore, we constructed phase portraits corresponding to different dynamical scenarios, illustrating the associated equilibria and parameter regimes.

The codimension-2 Bogdanov–Takens bifurcation in the discrete predator–prey model with a generalized Holling type-III functional response and a strong Allee effect marks a critical point in parameter space where the local population dynamics undergo a qualitative change. Near this point, small parameter variations can trigger transitions among dynamical regimes, including stable coexistence and oscillatory behavior. At the same time, changes in the stability and existence of equilibria may be linked to population decline. From a biological perspective, the interplay between nonlinear predation and a critical Allee threshold contributes to the complex local dynamics observed near the Bogdanov–Takens point. The results therefore suggest that this bifurcation point may be relevant to understanding potential regime shifts in the model. However, interpreting the Bogdanov–Takens point as an ecological tipping point in a broader empirical sense would require further biologically calibrated simulations and/or empirical evidence. The main contribution of this paper is the derivation of explicit parameter conditions and the systematic generation of phase portraits (Figures 2–9) based on numerical simulations for representative parameter values. Compared to existing studies, which often rely primarily on illustrative examples (e.g., Figure 8.8 in [22, p. 322]), our results provide a more complete characterization of the underlying bifurcation structure.

Use of AI tools declaration

The authors declare that they did not use Artificial Intelligence (AI) tools in the creation of this article.

Author contributions

All authors contributed equally to the conceptualization, methodology, formal analysis, investigation, and writing of the manuscript, including the original draft preparation and review and editing. All authors approved the final version of the manuscript.

Acknowledgments

The authors would like to thank the anonymous reviewers for their valuable comments and suggestions, which helped to improve the quality and presentation of this manuscript.

This work was supported by the Ministry of Education and Science of Tuzla Canton, Federation of

Bosnia and Herzegovina, under Grant No. 10/1-11-13074-2/26 dated June 25, 2026.

Conflict of interest

The authors declare no conflicts of interest.

References

1. E. Bešo, S. Kalabušić, E. Pilav, Fold-Flip and Bogdanov–Takens bifurcations of a discrete predator–prey system with cooperative hunting, *Int. J. Bifurcat. Chaos*, **35** (2025), 2550150. https://doi.org/10.1142/S0218127425501500
2. M. M. Bosschaert, Y. A. Kuznetsov, Bifurcation analysis of Bogdanov–Takens bifurcations in delay differential equations, *SIAM J. Appl. Dyn. Syst.*, **23** (2024), 553–591. https://doi.org/10.1137/22M1527532
3. L. Cheng, L. Zhang, Bogdanov–Takens bifurcation of a Holling IV prey-predator model with constant-effort harvesting, *J. Inequal. Appl.*, **2021** (2021), 68. https://doi.org/10.1186/s13660-021-02597-9
4. Q. Din, T. Donchev, D. Kolev, Stability, Bifurcation analysis and chaos control in Chlorine Dioxide-Iodine-Malonic acid reaction, *MATCH Commun. Math. Comput. Chem.*, **79** (2018), 577–606.
5. Q. Din, U. Saeed, Stability, discretization, and bifurcation analysis for a chemical reaction system, *MATCH Commun. Math. Comput. Chem.*, **90** (2023), 151–174. https://doi.org/10.46793/match.90-1.151D
6. Q. Din, M. Shabira, M. Khan, A cubic autocatalator chemical reaction model with limit cycle analysis and consistency preserving discretization, *MATCH Commun. Math. Comput. Chem.*, **87** (2022), 441–462. https://doi.org/10.46793/match.87-2.441D
7. T. Faria, L. T. Magalhães, Normal forms for retarded functional differential equations and applications to Bogdanov–Takens singularity, *J. Differ. Equations*, **122** (1995), 201–224. https://doi.org/10.1006/jdeq.1995.1144
8. H. I. Freedman, *Deterministic Mathematical Models in Population Ecology*, Pure and Applied Mathematics, Vol. 57, Marcel Dekker, New York, 1980.
9. M. Garić-Demirović, S. Hrustić, S. Moranjkić, M. Nurkanović, Z. Nurkanović, The existence of Li-Yorke chaos in certain predator–prey system of difference equations, *Sarajevo J. Math.*, **18** (2022), 45–62. https://doi.org/10.5644/SJM.18.01.04
10. M. Garić-Demirović, S. Moranjkić, M. Nurkanović, Z. Nurkanović, Stability, Neimark–Sacker bifurcation, and approximation of the invariant curve of certain homogeneous second-order fractional difference equation, *Discrete Dyn. Nat. Soc.*, **2020** (2020), 1–12. https://doi.org/10.1155/2020/6254013
11. G. F. Gause, N. P. Smaragdova, A. A. Witt, Further studies of interaction between predators and prey, *J. Anim. Ecol.*, **5** (1936), 1–18. https://doi.org/10.2307/1087

12. A. Goldbeter, *Biochemical Oscillations and Cellular Rhythms*, Cambridge Univ. Press, Cambridge, 1996.

13. A. B. Hamed, B. B. Hamed, Bogdanov–Takens bifurcation in a Hopfield network model with bidirectional connection and multiple delays, *IMA J. Math. Control Inform.*, **34** (2017), 111–122. https://doi.org/10.1093/imamci/dnv035

14. Z. He, W. Li, Complex dynamic behavior of a discrete-time predator–prey system of Holling-III type, *Adv. Differ. Equ.*, **2014** (2014), 180. https://doi.org/10.1186/1687-1847-2014-180

15. S. Hrustić, S. Moranjkić, Z. Nurkanović, Local stability, period-doubling and 1:2 resonance bifurcation for a discretized chemical reaction system, *MATCH Commun. Math. Comput. Chem.*, **93** (2025), 349–378. https://doi.org/10.46793/match.93-2.349H

16. J. Huang, S. Liu, S. Ruan, D. Xiao, Bifurcations in a discrete predator–prey model with nonmonotonic functional response, *J. Math. Anal. Appl.*, **464** (2018), 201–230. https://doi.org/10.1016/j.jmaa.2018.03.074

17. S. Jašarević Hrustić, M. R. S. Kulenović, M. Nurkanović, Global dynamics and bifurcations of certain second order rational difference equation with quadratic terms, *Qual. Theor. Dyn. Syst.*, **14** (2015), 283–307. https://doi.org/10.1007/s12346-015-0148-x

18. S. Kalabušić, E. Pilav, Bifurcations, Permanence and local behavior of the Plant-Herbivore model with logistic growth of plant biomass, *Qual. Theor. Dyn. Syst.*, **21** (2022), 52. https://doi.org/10.1007/s12346-022-00561-6

19. M. R. S. Kulenović, O. Merino, *Discrete Dynamical Systems and Difference Equations with Mathematica*, Chapman and Hall/CRC, Boca Raton, 2002.

20. M. R. S. Kulenović, S. Moranjkić, M. Nurkanović, Z. Nurkanović, Global asymptotic stability and Naimark–Sacker bifurcation of certain mixed monotone difference equation, *Discrete Dyn. Nat. Soc.*, **2018** (2018), 7052935. https://doi.org/10.1155/2018/7052935

21. M. R. S. Kulenović, S. Moranjkić, Z. Nurkanović, Naimark–Sacker bifurcation of second order rational difference equation with quadratic terms, *J. Nonlinear Sci. Appl.*, **10** (2017), 3477–3489. https://dx.doi.org/10.22436/jnsa.010.07.11

22. Y. A. Kuznetsov, *Elements of Applied Bifurcation Theory*, 2nd edition, Springer-Verlag, New York, 1998.

23. A. P. Kuznetsov, A. V. Savin, Y. V. Sedova, Bogdanov–Takens bifurcation: from flows to discrete systems, *Izvestiya VUZ. Appl. Nonlinear Dyn.*, **17** (2009), 139–158. https://doi.org/10.18500/0869-6632-2009-17-6-139-158

24. X. Liu, J. Wang, Bogdanov–Takens and triple zero bifurcations in general differential systems with delays, *Nonlinear Analysis: Modelling and Control*, **21** (2016), 731–750. https://doi.org/10.15388/NA.2016.6.1

25. A. J. Lotka, *Elements of Physical Biology*, Williams & Wilkins, Baltimore, 1925.

26. Z. Nurkanović, M. Nurkanović, M. Garić-Demirović, Stability and Neimark–Sacker bifurcation of certain mixed monotone rational second–order difference equation, *Qual. Theor. Dyn. Syst.*, **20** (2021), 41. https://doi.org/10.1007/s12346-021-00515-4

27. M. Ruan, C. Li, X. Li, Codimension two 1:1 strong resonance bifurcation in a discrete predator–prey model with Holling IV functional response, *AIMS Math.*, **7** (2022), 3150–3168. https://doi.org/10.3934/math.2022174

28. E. Sánchez, Indirect Allee effect, bistability and chaotic oscillations in a predator–prey discrete model, *Chaos, Soliton. Fract.*, **24** (2005), 85–101. https://doi.org/10.1016/j.chaos.2004.07.018

29. E. E. Selkov, Self-oscillations in glycolysis, *Eur. J. Biochem.*, **4** (1968), 79–86. https://doi.org/10.1111/j.1432-1033.1968.tb00175.x

30. M. Verma, A. Misra, Modeling the effect of prey refuge on a ratio-dependent predator–prey system with the Allee effect, *Bull. Math. Biol.*, **80** (2018), 626–656. https://doi.org/10.1007/s11538-018-0394-6

31. V. Volterra, Variazioni e fluttuazioni del numero d'individui in specie animali conviventi, *Memorie della R. Accademia Nazionale dei Lincei*, **2** (1926), 31–113.

32. Y. Xu, M. Huang, Homoclinic orbits and Hopf bifurcations in delay differential systems with T–B singularity, *J. Differ. Equations*, **244** (2008), 582–598. https://doi.org/10.1016/j.jde.2007.09.003

33. K. Yagasaki, Melnikov's method and codimension–two bifurcations in forced oscillations, *J. Differ. Equations*, **185** (2002), 1–24. https://doi.org/10.1006/jdeq.2002.4177

34. Y. Zeng, P. Yu, Multistable states in a predator–prey model with generalized Holling type III functional response and a strong Allee effect, *Commun. Nonlinear Sci.*, **131** (2024), 107846. https://doi.org/10.1016/j.cnsns.2024.107846

35. H. Zhang, Y. Liu, Stability and bifurcation of a discrete predator–prey system with Holling type III functional response, *Discrete Dyn. Nat. Soc.*, **2012** (2012), 162097.

Appendix A

Corresponding Taylor series coefficients.

$$
\begin{aligned}
A_{00}(\boldsymbol{\alpha}) &= a_{00}(\boldsymbol{\alpha}) - \left(\frac{1}{2}a_{10}(\boldsymbol{\alpha}) - \frac{1}{3}b_{10}(\boldsymbol{\alpha})\right)a_{00}(\boldsymbol{\alpha}) \\
&\quad - \left(\frac{1}{2} - \frac{1}{3}a_{10}(\boldsymbol{\alpha}) + \frac{1}{2}a_{01}(\boldsymbol{\alpha}) + \frac{1}{4}b_{10}(\boldsymbol{\alpha}) - \frac{1}{3}b_{01}(\boldsymbol{\alpha})\right)b_{00}(\boldsymbol{\alpha}), \\
A_{10}(\boldsymbol{\alpha}) &= a_{10}(\boldsymbol{\alpha}) - \frac{1}{2}b_{10}(\boldsymbol{\alpha}), \\
A_{01}(\boldsymbol{\alpha}) &= a_{01}(\boldsymbol{\alpha}) - \frac{1}{2}a_{10}(\boldsymbol{\alpha}) + \frac{1}{3}b_{10}(\boldsymbol{\alpha}) - \frac{1}{2}b_{01}(\boldsymbol{\alpha}), \\
A_{20}(\boldsymbol{\alpha}) &= a_{20}(\boldsymbol{\alpha}) - \frac{1}{2}b_{20}(\boldsymbol{\alpha}), \\
A_{11}(\boldsymbol{\alpha}) &= a_{11}(\boldsymbol{\alpha}) - \frac{1}{2}a_{20}(\boldsymbol{\alpha}) + \frac{1}{3}b_{20}(\boldsymbol{\alpha}) - \frac{1}{2}b_{11}(\boldsymbol{\alpha}), \\
A_{02}(\boldsymbol{\alpha}) &= a_{02}(\boldsymbol{\alpha}) + \frac{1}{6}a_{20}(\boldsymbol{\alpha}) - a_{11}(\boldsymbol{\alpha}) - \frac{1}{6}b_{20}(\boldsymbol{\alpha}) + \frac{2}{3}b_{11}(\boldsymbol{\alpha}) - \frac{1}{2}b_{02}(\boldsymbol{\alpha}),
\end{aligned}
$$

$$B_{00}(\boldsymbol{\alpha}) = b_{00}(\boldsymbol{\alpha}) - \frac{1}{2}b_{10}(\boldsymbol{\alpha})\,a_{00}(\boldsymbol{\alpha}) + \left(\frac{1}{3}b_{10}(\boldsymbol{\alpha}) - \frac{1}{2}b_{01}(\boldsymbol{\alpha})\right)b_{00}(\boldsymbol{\alpha}),$$

$$B_{10}(\boldsymbol{\alpha}) = b_{10}(\boldsymbol{\alpha}),$$

$$B_{01}(\boldsymbol{\alpha}) = b_{01}(\boldsymbol{\alpha}) - \frac{1}{2}b_{10}(\boldsymbol{\alpha}),$$

$$B_{20}(\boldsymbol{\alpha}) = b_{20}(\boldsymbol{\alpha}),$$

$$B_{11}(\boldsymbol{\alpha}) = b_{11}(\boldsymbol{\alpha}) - \frac{1}{2}b_{20}(\boldsymbol{\alpha}),$$

$$B_{02}(\boldsymbol{\alpha}) = b_{02}(\boldsymbol{\alpha}) + \frac{1}{6}b_{20}(\boldsymbol{\alpha}) - b_{11}(\boldsymbol{\alpha}).$$

Appendix B

Lemma 11. *Suppose that the following nondegeneracy conditions* $B_{20}(\mathbf{0}) = b_{20}(\mathbf{0}) \neq 0$ *and* $A_{20}(\mathbf{0}) + B_{11}(\mathbf{0}) \neq 0$ *are satisfied. Then under analytical changes of coordinates and scaling of the time, System (4.5) becomes*

$$\begin{cases} \dot{v}_1 = v_2, \\ \dot{v}_2 = \eta_1(\boldsymbol{\alpha}) + \eta_2(\boldsymbol{\alpha})\,v_1 + v_1^2 + s v_1 v_2 \end{cases}$$

up to $O\left(|v_1|^2 + |\boldsymbol{\alpha}|^2\right)$, *where*

$$s = sgn\left[B_{20}(\mathbf{0})\left(A_{20}(\mathbf{0}) + B_{11}(\mathbf{0})\right)\right] = \pm 1$$

and $\eta_1(\boldsymbol{\alpha})$ *and* $\eta_2(\boldsymbol{\alpha})$ *can be written as follows:*

$$\eta_1(\boldsymbol{\alpha}) = \frac{8\beta_0^4(\mathbf{0})}{B_{20}^3(\mathbf{0})}\beta_1(\boldsymbol{\alpha}) - \frac{8\beta_0^3(\mathbf{0})}{B_{20}^3(\mathbf{0})}\beta_2(\boldsymbol{\alpha})\beta_3(\boldsymbol{\alpha}) + \frac{4\beta_0^2(\mathbf{0})}{B_{20}^2(\mathbf{0})}\beta_2^2(\boldsymbol{\alpha}),$$

$$\eta_2(\boldsymbol{\alpha}) = \frac{4\beta_0^2(\mathbf{0})}{B_{20}^2(\mathbf{0})}\beta_4(\boldsymbol{\alpha}) - \frac{4\beta_0(\mathbf{0})}{B_{20}(\mathbf{0})}\beta_2(\boldsymbol{\alpha}),$$

with

$$\beta_0(\mathbf{0}) = a_{20}(\mathbf{0}) + b_{11}(\mathbf{0}) - b_{20}(\mathbf{0}) = A_{20}(\mathbf{0}) + B_{11}(\mathbf{0}),$$

$$\begin{aligned}\beta_1(\boldsymbol{\alpha}) = {} & b_{00}(\boldsymbol{\alpha}) - a_{00}(\boldsymbol{\alpha})\,b_{01}(\boldsymbol{\alpha}) - \frac{1}{2}a_{10}(\boldsymbol{\alpha})\,b_{00}(\boldsymbol{\alpha}) + a_{01}(\boldsymbol{\alpha})\,b_{00}(\boldsymbol{\alpha}) \\ & + \frac{5}{12}b_{00}(\boldsymbol{\alpha})\,b_{10}(\boldsymbol{\alpha}) - \frac{1}{2}b_{00}(\boldsymbol{\alpha})\,b_{01}(\boldsymbol{\alpha}) + \frac{1}{2}\left(\frac{1}{6}b_{20}(\mathbf{0}) - b_{11}(\mathbf{0}) + b_{02}(\mathbf{0})\right)a_{00}^2(\boldsymbol{\alpha}) \\ & - \left(\frac{1}{6}a_{20}(\mathbf{0}) - a_{11}(\mathbf{0}) + a_{02}(\mathbf{0}) - \frac{1}{12}b_{20}(\mathbf{0}) + \frac{1}{6}b_{11}(\mathbf{0})\right)a_{00}(\boldsymbol{\alpha})\,b_{00}(\boldsymbol{\alpha}) \\ & + \frac{1}{2}\left(\frac{1}{6}a_{20}(\mathbf{0}) - a_{11}(\mathbf{0}) + a_{02}(\mathbf{0}) - \frac{1}{8}b_{20}(\mathbf{0}) + \frac{5}{12}b_{11}(\mathbf{0}) - \frac{1}{4}b_{02}(\mathbf{0})\right)b_{00}^2(\boldsymbol{\alpha}),\end{aligned}$$

$$\beta_2(\boldsymbol{\alpha}) = a_{10}(\boldsymbol{\alpha}) - b_{10}(\boldsymbol{\alpha}) + b_{01}(\boldsymbol{\alpha})$$

$$+\left(\frac{1}{2}a_{20}(\mathbf{0})-a_{11}(\mathbf{0})-\frac{1}{2}b_{20}(\mathbf{0})+\frac{3}{2}b_{11}(\mathbf{0})-b_{02}(\mathbf{0})\right)a_{00}(\boldsymbol{\alpha})$$
$$-\left(\frac{1}{12}a_{20}(\mathbf{0})+\frac{1}{2}a_{11}(\mathbf{0})-a_{02}(\mathbf{0})-\frac{1}{12}b_{20}(\mathbf{0})+\frac{1}{12}b_{11}(\mathbf{0})\right)b_{00}(\boldsymbol{\alpha}),$$

$$\beta_3(\boldsymbol{\alpha})=b_{10}(\boldsymbol{\alpha})+\left(\frac{1}{2}b_{20}(\mathbf{0})-b_{11}(\mathbf{0})\right)a_{00}(\boldsymbol{\alpha})-\left(\frac{1}{2}a_{20}(\mathbf{0})-a_{11}(\mathbf{0})-\frac{1}{12}b_{20}(\mathbf{0})\right)b_{00}(\boldsymbol{\alpha}),$$

$$\beta_4(\boldsymbol{\alpha})=b_{10}(\boldsymbol{\alpha})+\left(\frac{1}{2}b_{20}(\mathbf{0})-b_{11}(\mathbf{0})\right)a_{00}(\boldsymbol{\alpha})$$
$$+\left(\frac{1}{2}a_{20}(\mathbf{0})-a_{11}(\mathbf{0})-\frac{3}{4}b_{20}(\mathbf{0})+2b_{11}(\mathbf{0})-b_{02}(\mathbf{0})\right)b_{00}(\boldsymbol{\alpha}).$$

Furthermore, if the transversality condition

$$\det J_{\boldsymbol{\alpha}}\boldsymbol{\eta}(\mathbf{0})\neq 0$$

is satisfied, then the above system is the versal unfolding of the Bogdanov–Takens singularity of codimension 2.



AIMS Press

© 2026 the Author(s), licensee AIMS Press. This is an open access article distributed under the terms of the Creative Commons Attribution License (https://creativecommons.org/licenses/by/4.0)